Feasibility Study of Leonardo da Vinci's Bridge Proposal over the Golden Horn in Istanbul

by

Karly Maria Bast

B.S. Civil and Environmental Engineering
University of Illinois at Urbana Champaign, 2018

Submitted to the Department of Civil and Environmental Engineering
in partial fulfillment of the requirements for the degree of

Master of Engineering in Civil and Environmental Engineering
at the
Massachusetts Institute of Technology

June 2019

Signature redacted

Author.....
Department of Civil and Environmental Engineering
May 10, 2019

Signature redacted

Certified by.....
John A. Ochsendorf
Class of 1942 Professor of Civil and Environmental Engineering and Architecture
Thesis Supervisor

Accepted by..... Signature redacted .....
Heidi Nepf
Donald and Martha Harleman Professor of Civil and Environmental Engineering
Chair, Graduate Program Committee

Feasibility Study of Leonardo da Vinci's Bridge Proposal over the Golden Horn in Istanbul

Karly Bast

Submitted to the Department of Civil and Environmental Engineering on May 10, 2019 in Partial Fulfillment of the Requirements for the Degree of Master of Engineering in Civil and Environmental Engineering

Abstract

This thesis investigates the feasibility of a masonry arch bridge proposed by Leonardo da Vinci (1452 -1519). Leonardo wrote a proposal in 1502-1503 for a masonry bridge spanning over the Golden Horn in present-day Istanbul, Turkey. The design was a response to an invitation by the Sultan Bayezid II (1447-1512) to construct a bridge connecting Galata and Istanbul. Had Leonardo's design been constructed, at a span of roughly 280 meters, it would have been the one of the longest spans in the pre-Industrial world.

This thesis examines Leonardo's proposal, assesses the proposed location and geometry, and determines the feasibility of the design through a structural analysis. As the proposed bridge is a masonry structure, the most critical structural factors include geometric stability and the response to support displacements. Both of these factors are tested through analytical means and a 3D physical model supported by moveable abutments. The combination of the initial stability, the kinematic mechanism under spreading supports, and the geotechnical conditions demonstrates the bridge's feasibility.

Thesis Supervisor: John A. Ochsendorf
Title: Class of 1942 Professor of Civil and Environmental Engineering and Architecture

Acknowledgements

I would first like to thank my advisor John Ochsendorf for advising me from across the Atlantic Ocean. Thank you, John for taking the time to inspire me and provide support for my academic and professional endeavors. It was an honor and privilege to work with you. Thank you for not only engaging me in a challenging topic, but also for guiding my learning with joy.

I would like to thank UROP student, Michelle Xie, for helping with the 3D modeling of the project and your support. Your collaboration in deciphering Leonardo's sketches and text were critical in this thesis and it would not have been possible without your expertise and dedication.

I would like to thank Doug Hamilton and his colleagues at PBS NOVA for their interest and support in this thesis topic.

Thank you to Stephen Rudolf and Jen O'Brien for your constant advising in the civil engineering shops and the architecture fabrication shop. It was a pleasure to work with you both and learn from you. Thank you for making this thesis possible.

Thank you to Professor Andrew Whittle and Michael Martello for your expertise in soil mechanics and foundation design. I sincerely appreciate the time you spent brainstorming with me and teaching me.

Thank you, Dr. James Bales for your assistance with the high-speed video camera and your willingness to teach.

Thank you to the CEE Academic Programs Office for your constant support and positive company.

I would like to thank the outstanding librarian staff at MIT for your active response and for providing all the literature necessary for the completion of this thesis.

I would also like to thank my fellow Master of Engineering students in Course 1. Your creativity and diverse knowledge base were an incredible asset while working on this thesis. You made this nine-month program full of adventure, laughs, and outstanding conversation.

Thank you to Professor Caitlin Mueller, Gordana Herning, and Josephine Carstensen for your inspiration. It was a privilege to learn from you and receive your feedback while working on this thesis.

Lastly, I would like to thank my family for their constant support throughout my academic, professional, and personal life these past nine months. It is a blessing to share this accomplishment with you.

Table of Contents

Symbols

CL: geotechnical acronym for low plasticity clay according to the Unified Soil Classification System (USCS)

CH: geotechnical acronym for high plasticity clay according to the USCS

MH: geotechnical acronym for high plasticity silt according to the USCS

ML: geotechnical acronym for low plasticity silt according to the USCS

q_{ult}: bearing capacity of soil

c': cohesion coefficient

ϕ': friction angle

E: elastic modulus

γ: unit weight

α : half angle of embrace

β : angle between the crown to the first intrado

σ : internal compressive stress

σ_{max} : compressive strength of a specified material

x : variable distance the right abutment moves horizontally

H : horizontal thrust of an arch

V : vertical reaction, the weight of the bridge

h : thickness of the arch at the crown

y : contact thickness at the crown of an arch

Chapter 1 - Introduction

Leonardo da Vinci (1452-1519) is known for his vast curiosities and influences across many disciplines. While Leonardo da Vinci was more significantly recognized for his contributions in art, biology, mechanics, and even astronomy, his novelties delved into the architecture and engineering world. His engineering contributions include a flying machine, a giant crossbow, scuba gear, and much more (Isaaccson 2017).

In particular, Leonardo proposed a bridge design to span over the Golden Horn in Turkey. As this bridge was never built, this thesis is the first case study of the structural behavior of the bridge as true to the design intention.

1.1 – Problem Statement

This thesis explores two fundamental questions:

(1) What was the proposed location and geometry?
(2) Was the bridge structurally feasible?

This thesis will build an understanding of the history and geometry of Leonardo's proposal, followed by a structural analysis of the bridge through theoretical expectations, experimental results, and geotechnical studies. The thesis will close with considerations regarding the bridge design's feasibility if it were to be built in its intended location.

1.2 – Literature Review

Between 1502 and 1503, the Sultan Beyazid II (1447-1512) of Turkey requested a design for a bridge to span over the Golden Horn (Nicholl 2004). Leonardo responded to this solicitation with a proposal, which was found in 1952 at the Topkapi Museum in Istanbul (Nicholl 2004). The translation from the original Italian proposal to English can be found in *The Literary Works of Leonardo da Vinci* (Pedretti and Richter 1977), replicated in Appendix A.

This written proposal begins with several promises to the Sultan and the bridge description is quite extravagant. Leonardo describes the bridge design as being as tall as a building so that boats can

easily pass through it without obstruction, but it will also contain a drawbridge (Pedretti and Richter 1977). Since Leonardo's proposal was perceived as ambitious, it was rejected by the Sultan and was not built.

In addition to the letter to the Sultan, there is a page from Leonardo's Paris Manuscripts L (Figure 1.1) now located in the Library of the Institute of France in Paris. This folio shows a sketch (Figure 1.2) and a caption (Figure 1.3) regarding Leonardo's bridge design over the Golden Horn. This folio provides clarity to the intention of his design through a visual representation of the bridge and annotation that describes the intended location and five key dimensions of the bridge.

In Leonardo's Paris Manuscripts L. folio 66, shown on the lower right in Figure 1.1, a plan and elevation view of the Galata bridge are sketched.

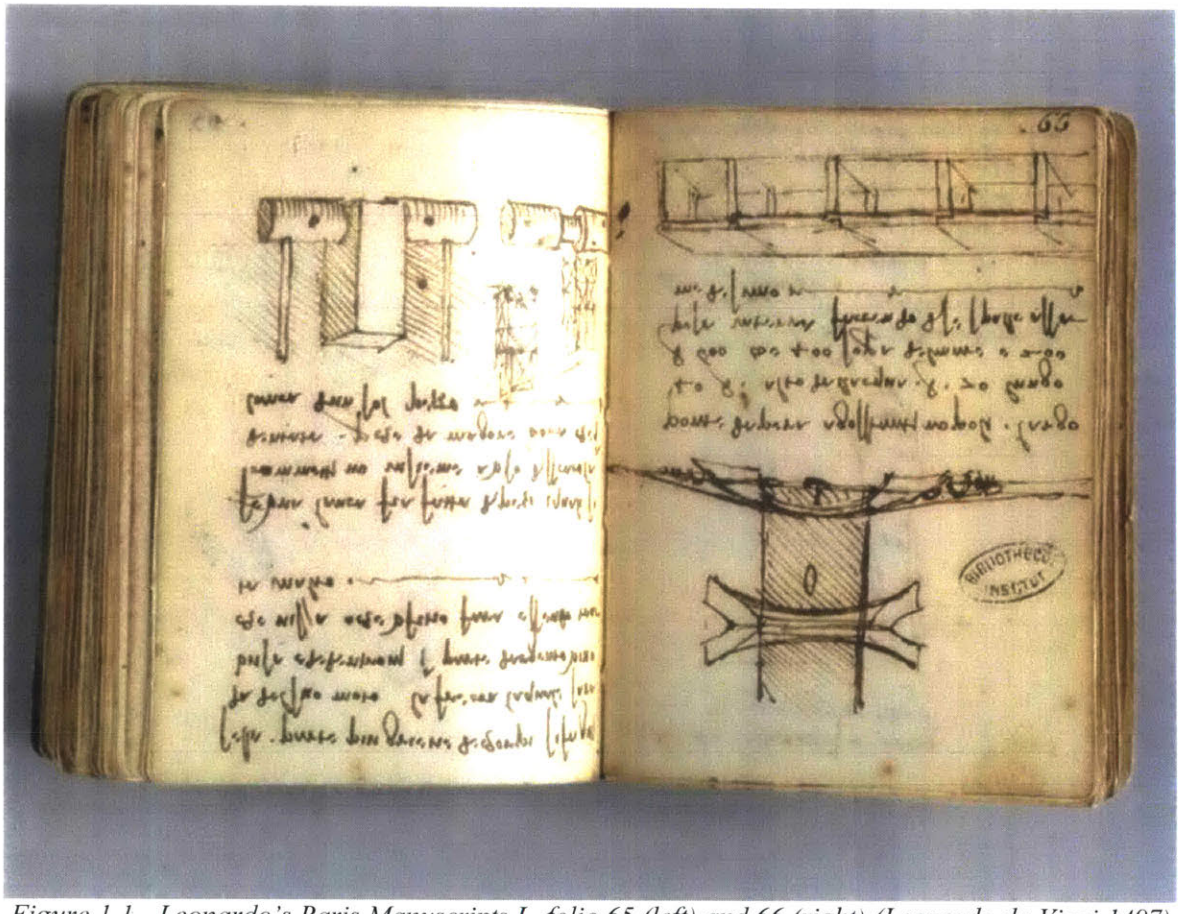

Figure 1.1 - Leonardo's Paris Manuscripts L. folio 65 (left) and 66 (right) (Leonardo da Vinci 1497)

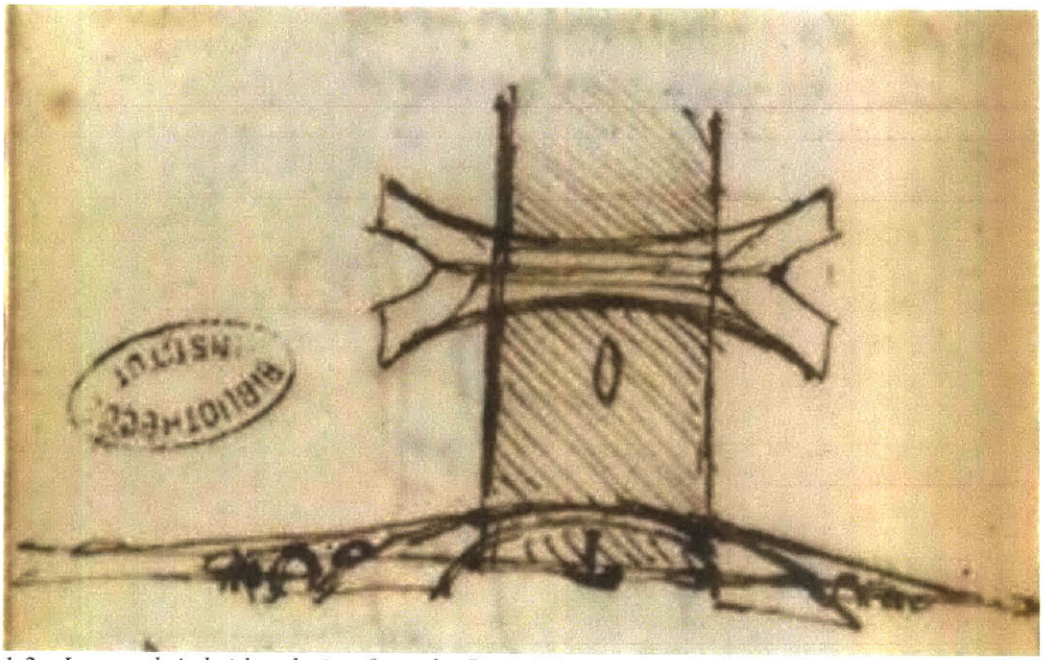

Figure 1.2 - Leonardo's bridge design from the Paris Manuscripts L. folio 66, flipped (Leonardo da Vinci 1497)

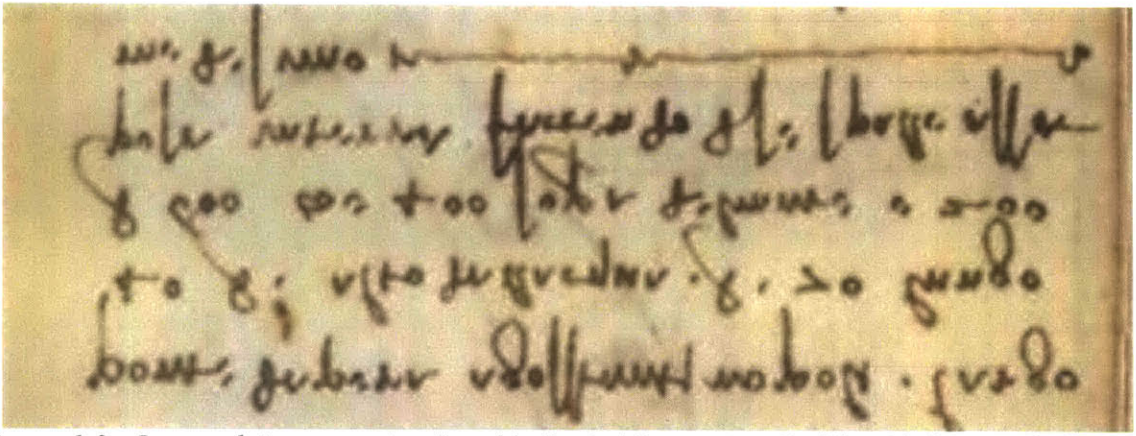

Figure 1.3 - Leonardo's annotation from his Paris Manuscripts L. folio 66 (Leonardo da Vinci 1497)

The translation of the text above the sketch presents a unique connection to the proposal found in 1952. The text shown in Figure 1.3 is common of Leonardo's annotations, such that the writing is presented in his upside down technique (Venerella 1999). The Italian translation is courtesy of Franco Schettini and is shown below:

"*Ponte da Pera a Constantinopoli, largo braccia 40, alto dall'acqua braccia 70, lungo braccia 600, cioè 400 sopra dal mare e 200 posa in terra facendo di sè spalle a se medesimo* (Schettini 1972)"

Likewise, the English translation is courtesy of John Venerella and is shown below:

"*Bridge from Pera to Constantinople, 40 braccia wide, 70 braccia high over the water, 600 braccia long, that is, 400 over the sea and 200 standing on the ground, providing its own support for itself. (Venerella 1999)*"

The term "braccia" refers to an early Italian unit of length, where its definition is dependent on the region in Italy from which it derives. For example, in Venice the braccia is equal to 0.683 meters, in Milan the braccia is equal to 0.595 meters, and in Florence the braccia is equal to 0.583 meters (Cardarelli 2003). For the purposes of this thesis, the braccia is taken to equal seven tenths of a meter. This then translates to roughly 28m wide, 49m high, 420m long, 280m over the water, and 140m standing on the ground.

In terms of the location, Pera and Constantinople are now known as Galata and Istanbul respectively (Kayra 1990).

Since Leonardo's annotations and meaning of his sketch have been connected to his bridge proposal over the Golden Horn, it inspired the design of a smaller scaled wooden and stainless-steel pedestrian bridge was built in Norway in 2001 (Nicholl 2004). While this bridge was designed based on Leonardo's proportions, it was built at a smaller scale, used materials not available during Leonardo's time, and was built at a different site than intended. It is also a contemporary design which is not a masonry arch bridge and does not act primarily in compression.

Thus, the purpose of this thesis will be to decipher Leonardo's design and study its feasibility. This will be accomplished through an analysis of his drawing to establish the intended geometry. Then a structural analysis of this geometry will be done through theoretical means, a physical model experiment, and geotechnical considerations.

Chapter 2 - History and Geometry

There are two primary pieces of information that are connected to Leonardo's bridge design over the Golden Horn: the written proposal to the Sultan found in 1952, and his sketch and annotation from his manuscript. The written proposal provides information about the purpose of the bridge, while the sketch provides information about the geometry and location of the bridge. As such, the sketch and its annotation are of interest and will be used to attempt to decipher the bridge geometry.

As shown in Figure 2.1, Leonardo's design shows two visual definitions of the bridge: a view where the bridge is parallel to the water and the other that is perpendicular to the water. This interpretation is consistent with the drawing of the boat on the water; in the bottom drawing the boat is underneath the bridge, seen from elevation, while in the plan view the boat is parallel to the water, shown in Figure 2.1. These two separate views are connected through the boundaries of the water, which confirms this sketch is two different views of the same bridge: one in plan and one in elevation.

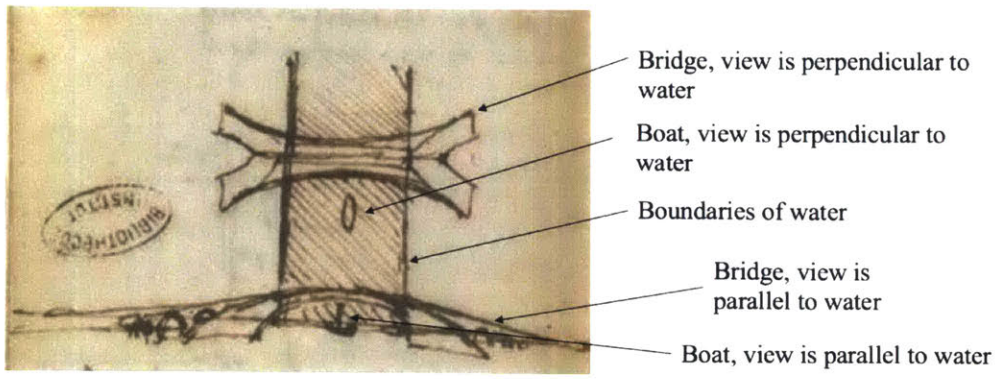

Figure 2.1 –Bridge orientation (After Leonardo da Vinci 1497)

Now that the orientation of the two different bridge views is established, the connection to the annotation will help define the overall geometry of the bridge.

As aforementioned from Venerella's translation of Leonardo's annotations, five dimensions of the bridge are known: 28 m wide, 49 m high, 420 m long, 280 m over the water, and 140 m standing on the ground (Venerella 1999). The first four dimensions will be used to calibrate the drawing

and define which lines define the outline of the bridge. The fifth dimension that will not be used is the 140 m standing on the ground because it refers to the difference between the long span and the span over the water.

By assuming that sketch is drawn at a consistent scale and by measuring from the drawing, it is possible to compare the numerical measurements given in the text with the scaled dimensions from the drawing.

Shown in Figure 2.2 are the four calibrations of Leonardo's sketch. The measured values according to the calibration are listed in Table 2.1.

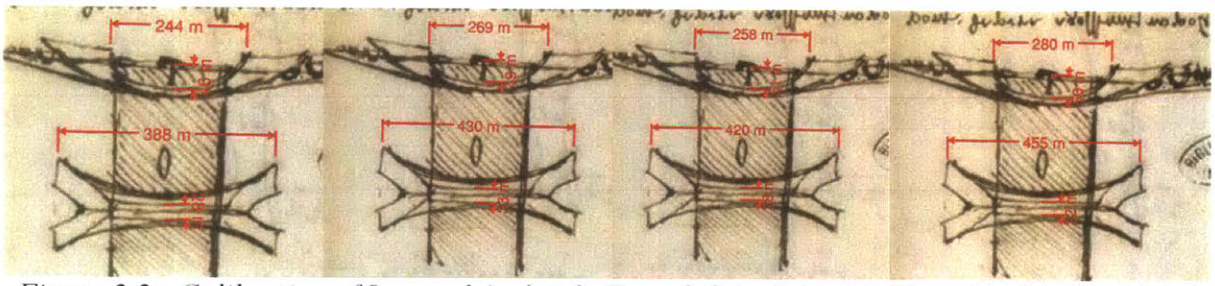

Figure 2.2 - Calibration of Leonardo's sketch. From left to right: (a) 28m wide (b) 49m high (c) 420m long (d) 280m standing on the ground

Table 2.1 – Calibration of each dimension and percent error

Measurement	Text Translated (m)	280m Calibrated (m)	420m Calibrated (m)	49m Calibrated (m)	28m Calibrated (m)	Error (m)	Error (%)
Short Span	280	280	258	269	244	+/- 36	13%
Long Span	420	455	420	430	388	+/- 35	8%
Height	49	56	51	49	46	+/- 7	14%
Width	28	32	28	33	28	+/- 5	18%

The error is calculated based on the maximum difference between the measured value and the given value from Leonardo's translated annotation. The percent error is the percentage of the error over the given value.

According to the Institute of France in Paris, folio 65 and 66 are 0.109 m tall and 0.072 m wide combined. Considering the size of the folios and the highest percent error being 18%, this is a reasonable amount of error for the size of the sketch. Not only does this validate the dimensions

from Leonardo's annotation, but it allows other critical dimensions to be measured from the sketch. For example, Leonardo's annotation does not define the thickness at the crown or the width at the abutments, but since the sketch is a scaled drawing these values can be measured.

A key component in understanding the geometry of the bridge is the definition of the bridge width. In Leonardo's annotation, only one dimension is given for the bridge width, 28 m. At a first glance, it seems that the only definition of the bridge width is the curved outline and that the lightly drawn lines on the inside are irrelevant. These lines are defined in Figure 2.3.

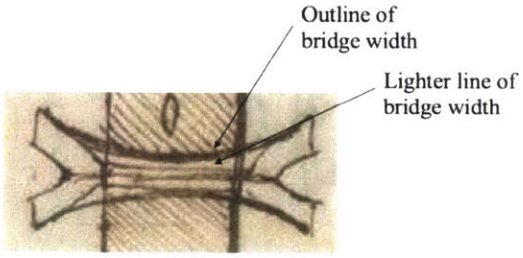

Figure 2.3 - Annotation of bridge and its width

But when using the height, and two length dimensions to calibrate the drawing, it is clear that the 28 m refers to the straight, lightly drawn lines on the inside of the curved outline, as shown in Figure 2.2. Therefore, the lightly drawn lines are defining the bridge width at 28 m, and the curved outlines must be a projection of the bridge width at a different elevation.

Connecting the plan view and elevation view in Figure 1.2, it is then clear that the curved outlines are at a higher elevation than the lightly drawn straight lines. Thus, the top sketch in Figure 1.2 is a footprint of the bridge, where the arch outline is at a higher elevation than the straight lighter lines. The notion that the plan view is a footprint of the bridge is confirmed by the lines defining the bridge abutment. Lines defining the bridge abutments would not appear in a top-down view but would appear in a footprint.

After each curve is generated as a parabolic curve using three points in its definition, a computer model is made. Figure 2.4 shows the interpreted geometry and dimensions of the bridge that are utilized for the three-dimensional model.

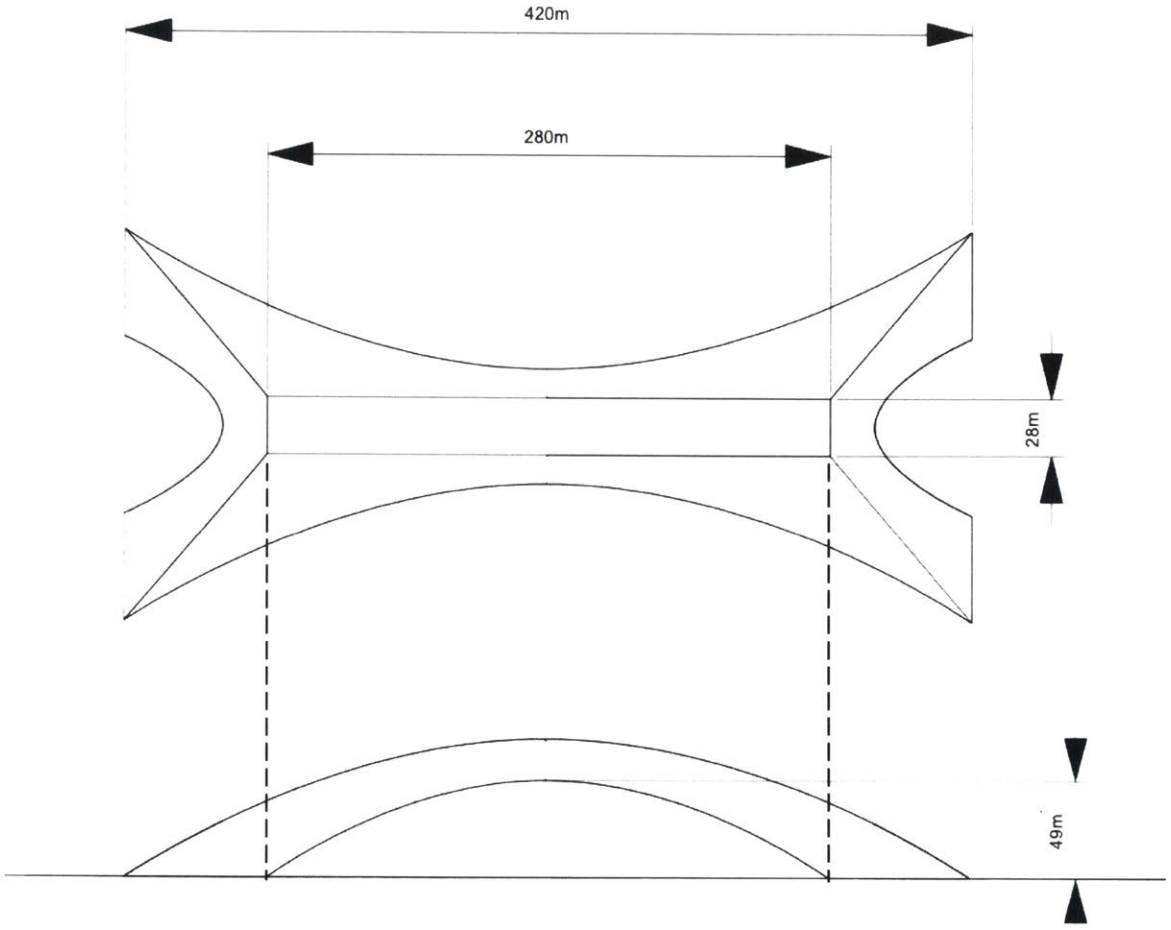

Figure 2.4 - Dimensioned footprint of the bridge. Top – Footprint of the bridge. Bottom – Elevation of the bridge

The two-dimensional drawings in Figure 2.4 are analyzed to project a three-dimensional model shown in Figure 2.5.

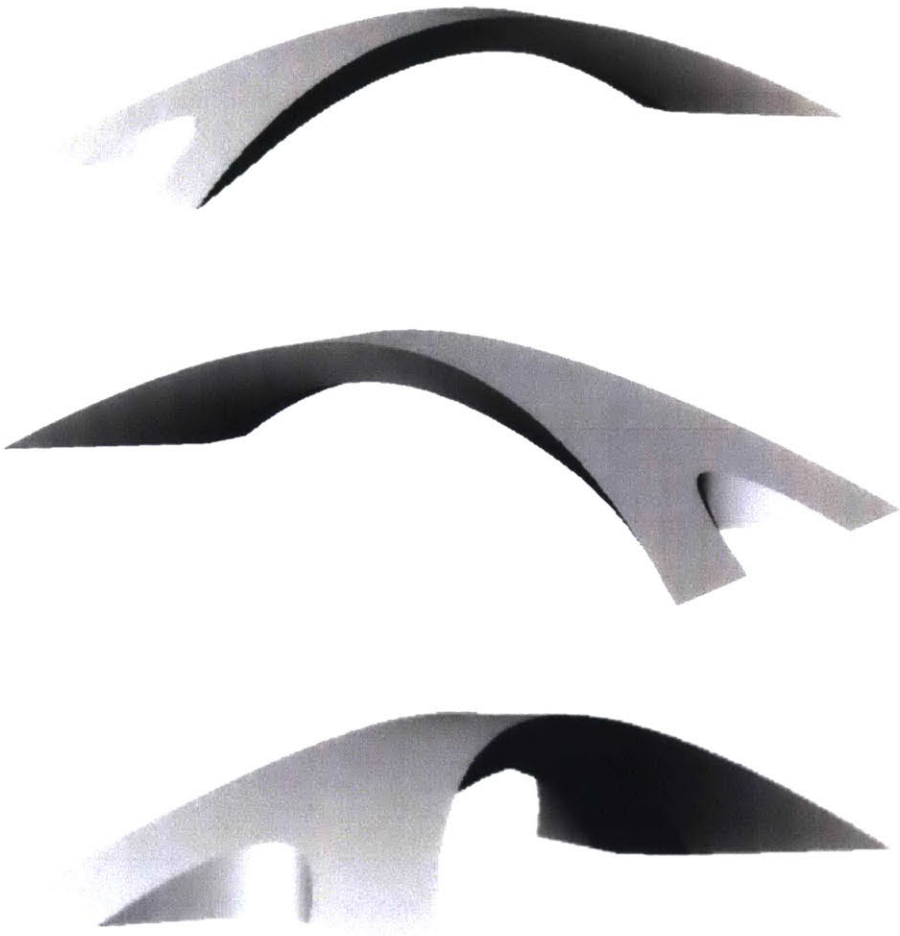

Figure 2.5 - Three-dimensional isometric views (Courtesy of Michelle Xie)

In this chapter, the geometry of Leonardo's bridge to span over the Golden Horn was deciphered using his sketch and annotation from folio 66 of his Paris manuscripts. The translation of the annotation lead to verification of the scale of the sketch. Through understanding the plan view of his sketch as a footprint, the three-dimensional geometry was interpreted.

Chapter 3 - Structural Feasibility

Now that the geometry of the bridge is established, the structural feasibility can be assessed. The structural feasibility is first assessed through theoretical means, where it is checked for structural stability based on its geometry and material stresses. Then, through a 1:500 scale physical model, its stability is tested for its initial geometry, and its behavior with spreading support conditions. Lastly, the geotechnical conditions are considered to assess the feasibility of the bridge at its intended site.

3.1 – Theory

In order to properly assess the structural behavior of the bridge, it is necessary to know the material of which it is made. Since the material of the bridge was not specified in Leonardo's letter or sketch, it is historically sound to treat the bridge as a masonry arch structure since bridges in the 16th century were commonly made of masonry: stone or brick (O'Connor 1993). Therefore, this chapter will pay attention to the initial geometry of the structure, check its material stresses, and predict its response under support displacements.

Initial Geometry

The following common assumptions are used for the initial equilibrium analysis (Heyman 1995):

- Masonry has no tensile strength
- Stresses in the structure are small compared to compressive strength of material
- Sliding failure does not occur between the voussoirs

The first assumption requires that each voussoir of the bridge must be in compression in order for stability to occur, which is conservative since masonry is weak in tension. The second assumption will be checked throughout the analysis to ensure it is correct but is typically true. The last assumption is reasonable since the friction between voussoir is usually very high (Ochsendorf 2002).

A common tool used to assess the stability of a masonry arch is the thrust line, which represents the compressive load path of the structure traveling between voussoirs. If the thrust line is

contained within the bounds of the structure, it is in equilibrium. The principle of the thrust line analysis is based on plastic theory, which states that if a state of equilibrium can be found for a load case then the structure is safe for that load case (Heyman 1995). Due to the heavy self-weight of masonry arches, this is taken to be the governing load case. Using equations of global equilibrium of the arch, local equilibrium of each voussoir, and graphic statics, the thrust line can be as shown in Figure 3.1.

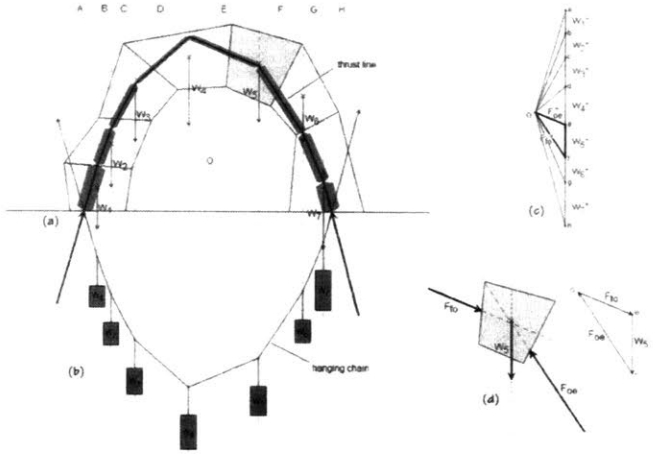

Figure 3.1- Graphical representation of global and voussoir equilibrium (Allen et al. 2010)

Leonardo's bridge is discretized into 22 voussoirs, as shown below in Figure 3.2, in order to simplify the problem and determine the location of the thrust line. In reality, the bridge would have been constructed with thousands of stones or millions of bricks. The discretization of the bridge into 22 voussoirs allows a reasonable approximation of the thrust line. It is important to note that voussoir 0 and 21 are independent of the arch and are considered to bear directly on the ground.

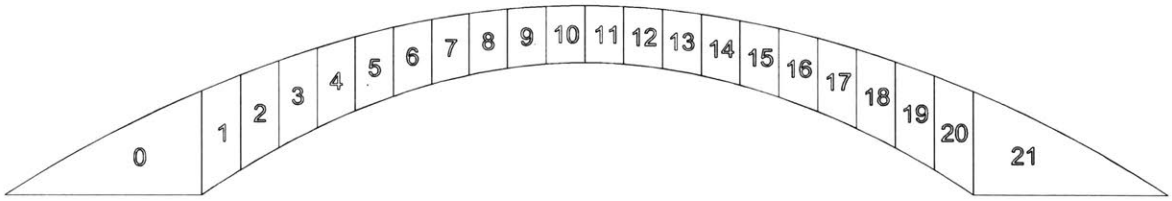

Figure 3.2 – Bridge discretized into 22 voussoirs. Voussoir 0 and 21 bear directly on ground.

The arch of interest includes 20 voussoirs, with each voussoir weight dependent on its volume and density of material. Table 3.1 shows the density of brick and stone before the 16th century to get an idea of the material properties that would have been available. The brick density used is from bricks from the Hagia Sophia (Moropoulou et al. 2002). The stone density used belongs to travertine, a type of limestone, from the Roman bridge Ponte di Augusto (Bertolesi et al. 2017). The voussoir weights are calculated and shown in Table 3.2. The free body diagram is shown in Figure 3.3.

Table 3.1 – Material densities

Material	Density (g/cm^3)
Brick	1.59 (Moropoulou et al. 2002)
Travertine	2.117 (Bertolesi et al. 2017)

Table 3.2 – Volume and weight of voussoirs

Voussoir No.	Volume (m^3)	Brick Weight (kN)	Stone Weight (kN)
0 and 21	165,000	2,580,000	3,400,000
1 and 20	56,000	876,000	1,167,000
2 and 19	46,000	719,000	958,000
3 and 18	38,000	593,000	789,000
4 and 17	31,500	492,000	655,000
5 and 16	26,500	413,000	550,000
6 and 15	22,600	353,000	470,000
7 and 14	19,700	308,000	410,000
8 and 13	17,700	276,000	367,000
9 and 12	16,400	256,000	341,000
10 and 11	15,800	246,000	328,000
Bridge Total	912,000	14,220,000	19,000,000

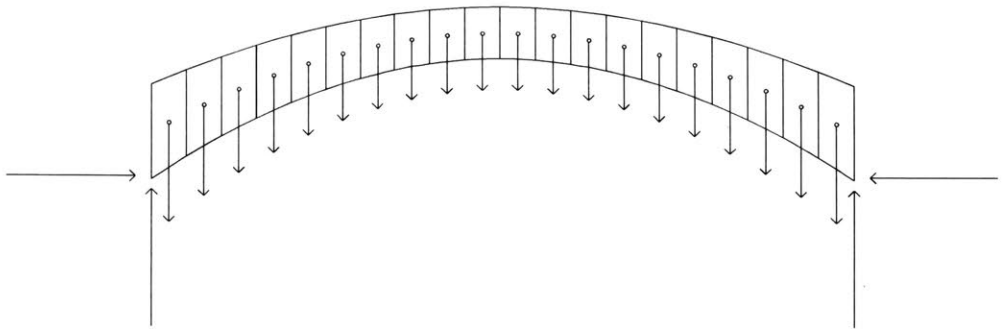

Figure 3.3– Free body diagram of the bridge

Similar to the graphic statics technique shown in Figure 3.1, the thrust line of Leonardo's bridge is calculated with two additional assumptions: there is low uniform stress at the crown and the thrust line acts at the interior of the support. The former assumption will be checked in the following section. The latter corresponds to a minimum thrust state at the supports and this assumption will be reviewed in the "Spreading Supports" section. Additionally, the arch is an indeterminate structure and there are infinite possible thrust lines. The thrust line shown in Figure 3.4 is one of the many possible thrust lines for the arch and Table 3.3 shows the support reactions.

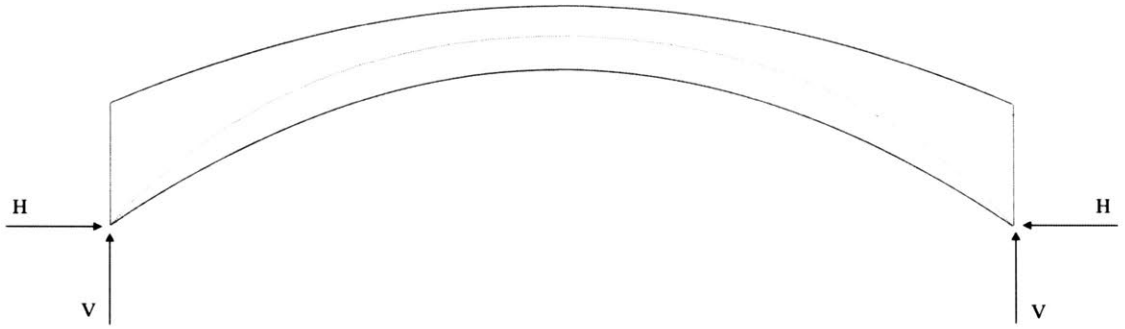

Figure 3.4– Thrust line of bridge shown in dotted line within the structure

Table 3.3 – Support reactions

Material	H (kN)	V (kN)
Stone	5,400,000	6,000,000
Brick	4,100,000	4,500,000

As a thrust line is found to be within the bounds of the structure, the structure is in equilibrium and is stable.

Stress Conditions

While the stability of masonry structures is usually governed by geometry and can be assessed by the location of the thrust line, it is also possible for the crushing stress of the material to be critical when the span is large (Heyman 1969). Because of the exceptionally long span of the Leonardo arch bridge proposal, it is important to verify that the maximum stress could be supported by the material.

For this long span masonry bridge, three stress distribution assumptions at the crown of the arch will be considered: uniform stress, uniform crushing stress, and triangular stress. When the material stresses in the bridge are significantly lower than the compressive strength of the material, the bridge is considered feasible in that material.

The stresses at the crown are controlling compared to the stresses at the springing because the cross-sectional area at the crown is significantly lower than the cross-sectional area at the springing of the arch. Though the forces are higher at the springing, the stresses are lower than at the crown due to this considerable difference in cross-sectional area.

The bridge is modeled as two-hinged arch under its own self weight, similar to the conditions for the thrust line calculation. Since stress is material dependent, the feasibility will be checked for both stone and brick with compressive strengths shown in Table 3.4.

Table 3.4 – Material compressive strengths

Material	Compressive Strength (kN/m^2)
Brick	5,100 (Ispir and Ilki 2013)
Stone	40,000 (Heyman 1995)

(1) Uniform Stress

The uniform stress distribution assumption is valid for material experiencing stresses well below its ultimate crushing strength. This condition is typical for stable masonry arches that have not undergone any significant deformation from their original position and have not experienced significant horizontal displacement at the supports.

This stress distribution is visualized in Figure 12, where only half of the arch is shown to visualize the internal stress. Through global equilibrium, the support reactions and the value of the uniform stress at the crown are calculated, where v_i, is the weight of voussoir i, H is the horizontal thrust at the support, V is the vertical reaction at the support, and σ is the uniform stress at the crown needed for equilibrium.

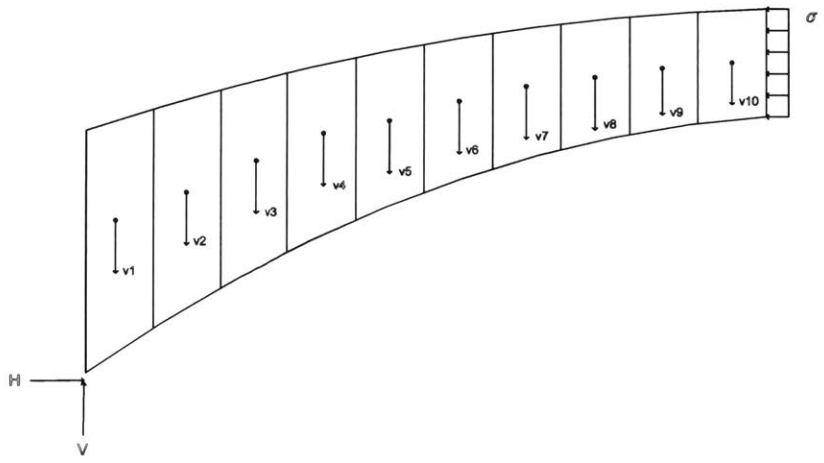

Figure 3.5- Uniform stress distribution free body diagram for half the bridge

Table 3.5 – Results for uniform stress distribution assumption

Material	H (kN)	V (kN)	σ_{max} (kN/m^2)	σ (kN/m^2)	$\sigma < \sigma_{max}$?
Stone	5,400,000	6,000,000	40,000	9,100	YES
Brick	4,100,000	4,500,000	5,100	6,800	NO

The stress experienced by the stone is less than that of the stone's ultimate strength and therefore the uniform stress assumption is in equilibrium for stone. As for brick, the stress exceeds the material strength and therefore is not feasible in brick for the uniform stress assumption.

(2) Uniform Crushing Stress

The uniform crushing stress distribution assumption is valid for when the arch has undergone horizontal deformation at the supports such that a hinge is beginning to develop at the crown and area of contact between the two halves is reduced. Through global equilibrium, the support reactions are calculated. The thickness of contact at the crown is iterated until the thrust at the crown equals the thrust at the support.

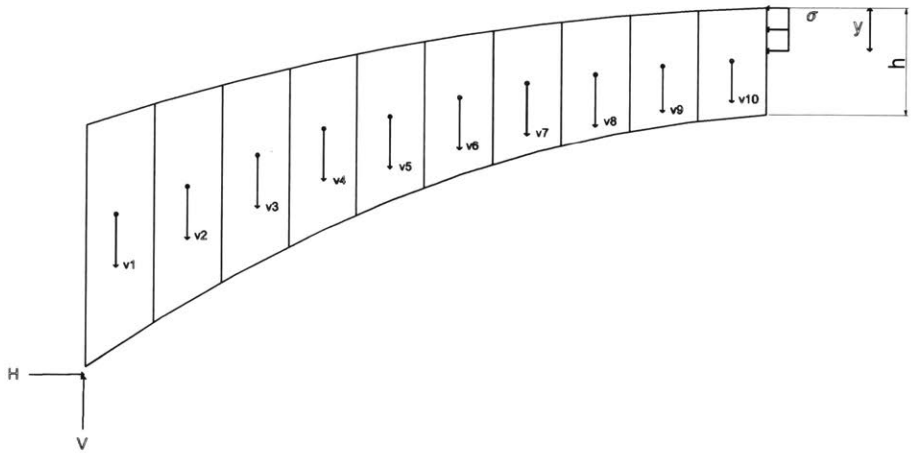

Figure 3.6- Uniform crushing stress distribution free body diagram for half the bridge

Table 3.6 – Results for uniform crushing stress distribution assumption

Material	H (kN)	V (kN)	h (m)	y (m)	y < h?
Stone	4,700,000	6,000,000	20	4.20	YES
Brick	4,400,000	4,500,000	20	30.7	NO

As the area of contact required to keep the bridge in equilibrium is less than that of the thickness at the crown for stone, the bridge is in equilibrium for the uniform crushing stress assumption for stone. For brick, the required area of contact to keep the bridge in equilibrium is greater than that of the thickness at the crown for brick and is therefore not feasible for the uniform crushing stress assumption.

(3) Triangular Stress Distribution

The triangular stress distribution assumption is valid for when the arch has undergone significant horizontal deformation at the supports such that a hinge is developing at the crown and there is minimal contact between the two halves of the arch. The support reactions and the thickness of contact at the crown is found similarly to the uniform crushing stress distribution assumption through iterative calculations.

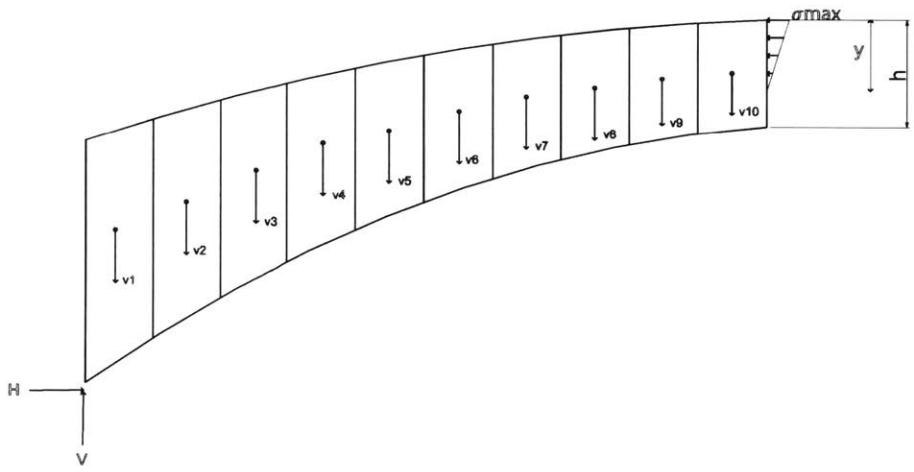

Figure 3.7- Triangular distribution free body diagram for half the bridge

Table 3.7 – Results for triangular stress distribution assumption

Material	H (kN)	V (kN)	h (m)	y(m)	y < h?
Stone	4,700,000	6,000,000	20	8.50	YES
Brick	5,300,000	4,500,000	20	74.0	NO

The area of contact required to keep the bridge in equilibrium is less than that of the thickness at the crown for stone. Therefore, the bridge is in equilibrium for the triangular stress assumption for stone. On the other hand for brick, the required area of contact to keep the bridge in equilibrium is greater than that of the thickness at the crown and is therefore not feasible in for the triangular stress assumption.

The conclusion of this analysis demonstrates that the stone maintains an acceptable level of compressive stress for all three stress distribution assumptions, while the crushing strength of the brick is not suitable for any of the assumptions. It is unusual for a masonry arch bridge to be governed by the strength of the material, but because of the immense scale of Leonardo's proposal, the compressive material stresses are quite high. While the thrust line in Figure 3.4 remains within the bounds of the structure for both materials, this is only true for when the stresses in the material are significantly below the material's crushing strength (Heyman 1995). Thus, the bridge shall be in equilibrium only if made of stone.

Spreading Supports

The stability of masonry structures is typically governed by geometry. While the initial geometry of a masonry arch can be stable, the movement of the supports may cause the geometry to change. The greatest risk to the stability of the structure is the gradual movement of the supports and deviation from the initial geometry (Ochsendorf 2002). Thus, it is possible for structures that are stable for hundreds of years to undergo collapse due to the uneven settlement of the structure's supports (Heyman 1995). In order to understand the stability of a masonry arch it is critical to not only understand its kinematic mechanism but predict the allowable displacements until its collapse.

The analysis of kinematic mechanisms for masonry arches on spreading supports has been studied by Ochsendorf (2006) for common arch geometries. As the supports move apart, the thrust line of the arch changes and the geometry of the arch adjusts in the form of hinges to allow the thrust line to remain within its boundaries. While the arch narrows, the thrust force at the support increases until collapse.

Ochsendorf (2002) was able to analyze the collapse behavior of masonry circular arches based on their thickness ratio, t/r, and angle of embrace, α as shown in Figure 3.8.

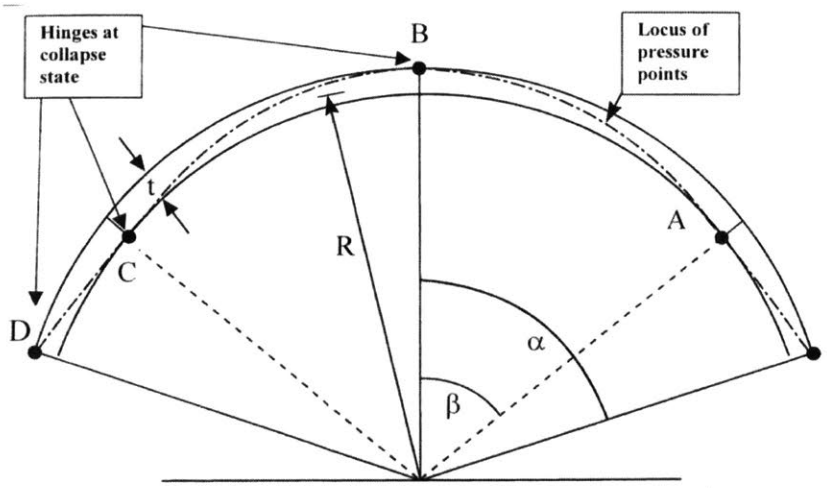

Figure 3.8 – A symmetric five-hinge mechanism for a circular arch (Ochsendorf 2002)

In order to understand if the arch will generate a five-hinge collapse, common for thinner arches, or a three-hinge collapse, common for thicker arches, it is necessary to find where the intrado hinges occur. The hinge location is defined by β, the angle between the crown to the first intrado hinge.

Ultimately, when the abutments start to spread apart and a hinge forms at the crown, it experiences its minimum thrust. As the abutment continues to move horizontally, the crown drops and the thrust increases. It can be expected that the intrado hinge occurs at the location that produces the highest minimum thrust. A three-hinge mechanism forms when the intrado hinge occurs at the abutment, otherwise a five-hinge mechanism forms. Both conditions create a statically determinate structure since the hinges provide one potential load path.

When the locations of the hinges are found and the kinematic mechanism is known, it is assumed that the collapse follows a rigid body deformation, where the hinge locations do not change. This can only be true for when the material stresses are low and the material can be assumed to have infinite compressive strength. For the 1:500 scale model this assumption is reasonable since the model is not so heavy. On the other hand, as shown in the previous section, the material stresses in the full-scale bridge are not low. So, stresses will most likely govern and the hinges can be expected to move in the full scale bridge; the hinge at the crown will move down and the hinges at the support will move up. As such, the expected kinematic mechanism for the full-scale bridge can only be a rough estimate, while for the 1:500 model it should be more accurate.

Assuming rigid-body deformation after the formation of the first hinges, the allowable horizontal displacement until collapse is completely based on geometry, where snap-through occurs when the crown can no longer be a single point and the two interior rigid bodies must disconnect.

In regard to Leonardo's bridge, several hinge locations are tested. The minimum thrust line is computed, where the angle of embrace is calculated from the radius of curvature to be $\alpha = 48^{o}$.

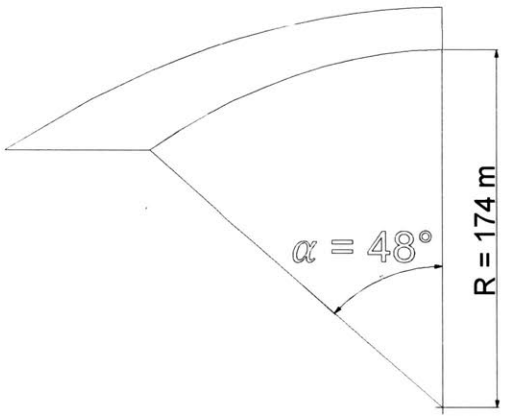

Figure 3.9 – Angle of embrace shown as $\alpha = 48^{o}$ based on curvature of arch (after Ochsendorf 2002)

To solve for the location of maximum minimum thrust, the minimum thrust is computed starting at $\beta = 48^{o}$. Then, as β decreases the minimum thrust is recalculated. The results are shown below:

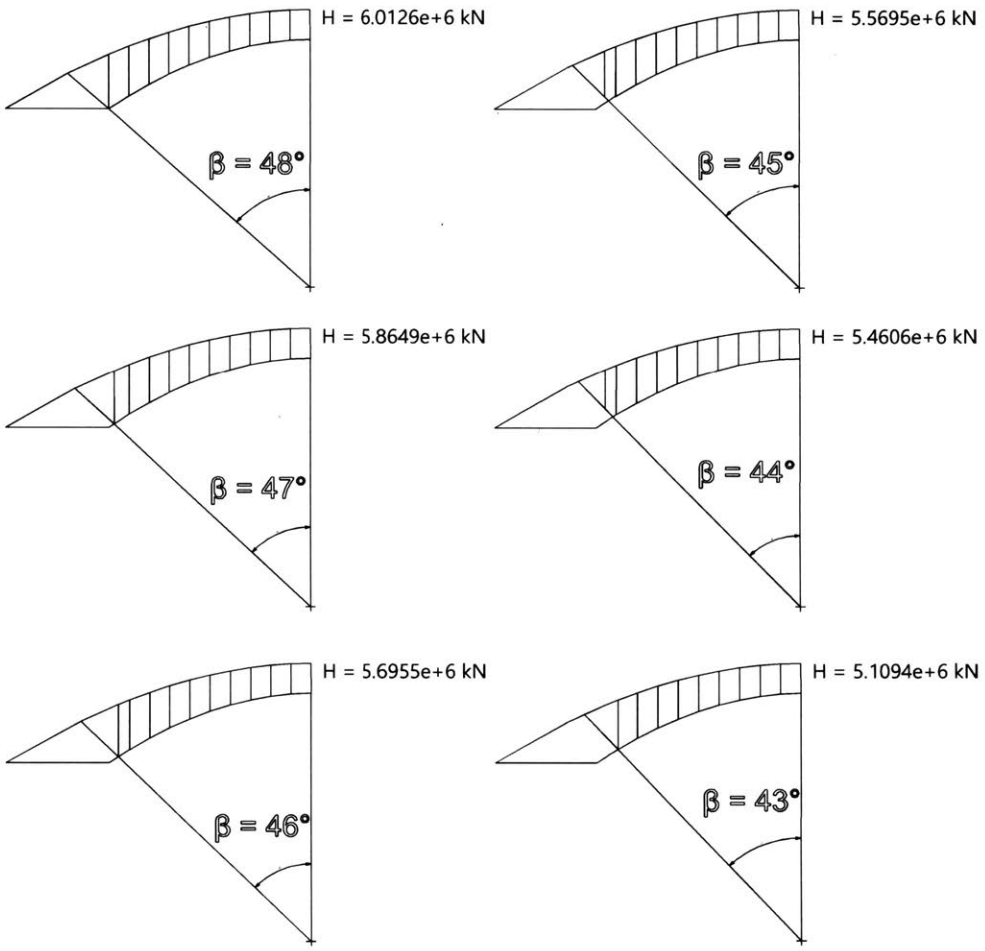

Figure 3.10– Minimum thrust calculation as a result of decreasing β

Figure 3.10 demonstrates that the maximum minimum thrust occurs when a $\beta = \alpha$, revealing that the intrado hinges are expected to occur at the abutments (Ochsendorf 2002).

Based on this relationship, a three-hinge is expected as one abutment moves horizontally. The three-hinge kinematic mechanism is shown in Figure 3.11, where x is the variable distance the right abutment moves horizontally.

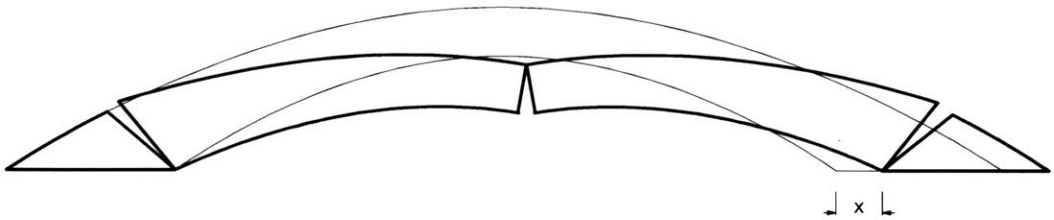

Figure 3.11 - Predicted three-hinge collapse mechanism, where x is the variable distance the right abutment moves horizontally

Since rigid body deformation is assumed, a snap-through failure is expected, where x keeps increasing until the crown can no longer be one point. This value of x is found through geometry, where both sides of the arch rotate about the abutment until the point where the arches meet lies on the horizontal. This mechanism is shown in Figure 3.12 for the full-scale bridge.

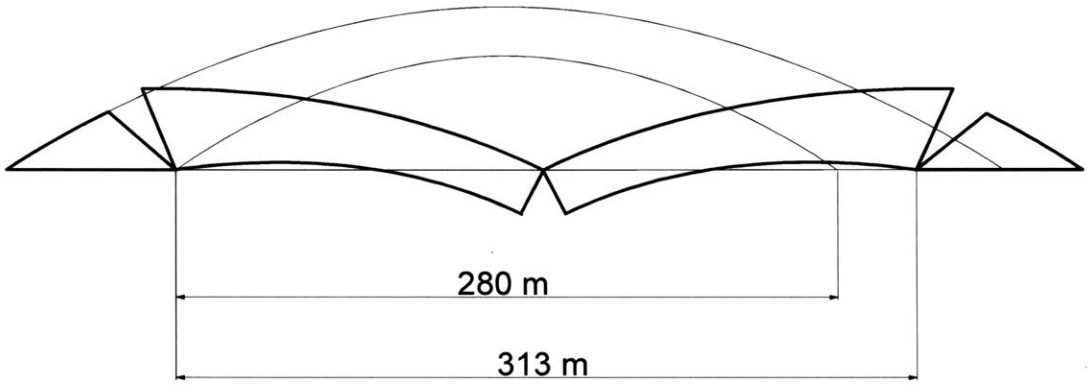

Figure 3.12 – Snap through failure of the full-scale bridge with a three-hinge kinematic mechanism

The value of x needed for a snap through failure is shown for the full-scale bridge and 1:500 scale model in Table 3.8.

Table 3.8 – Predicted displacements before collapse

Scale	Predicted displacement before collapse, x
1:1	33 m
1:500	66 mm

3.2 – Experiment

Since masonry structures are typically driven by geometric stability, small-scale models have become an inexpensive technique to accurately observe their collapse mechanisms (Quinonez et al. 2010; Shapiro 2012). Not only is the modeling relevant for structural behavior but it also allows designers to interact with the construction of the structure. In this chapter, a 1:500 scale 3D-printed model is designed and constructed to determine the bridge's initial stability and observe its behavior subjected to spreading supports.

Designing and Constructing the 3D model

Leonardo did not discretize the bridge into voussoirs for his design. Therefore, general principles of arch construction are used to split the bridge into stones for the 1:500 scale model. It is important to note that this discretization is highly dependent on the scale of the model so that the model can be constructed according to its 3D printing requirements. For example, for the 1:500 scale model it is reasonable to split the bridge into a few hundred voussoirs, but the full-scale bridge will require many more voussoirs to construct the bridge since the stones can only be so large.

In the past, 3D powder printing has been a powerful tool to model masonry structures. Quinonez et al. (2010) explored the use of powder 3D printing and its accuracy for modeling unreinforced masonry structures. Shapiro (2012) applied this methodology to explore the collapse behavior of unreinforced masonry barrel vault and groin vault. While the powder 3D prints model masonry behavior well, if pieces are too small or too large, they can lose precision or break. Therefore, it is important to consider the 3D printing limitations before designing the voussoir.

As such, ZCORP 3D printer expert, Jen O'Brien from the MIT Fabrication Laboratory, advised to limit each voussoir length to not be smaller than 1" or larger than 4" (25 to 100 mm). This was considered in the discretization of the voussoir.

Now that the size limitations of the voussoir are known, the orientation of the voussoir cuts can be made. After many iterations and collaboration with UROP MIT student, Michelle Xie, it was found that two layers for the elevation view and three layers for the plan view are ideal for this scale. The results are shown below in Figure 3.13.

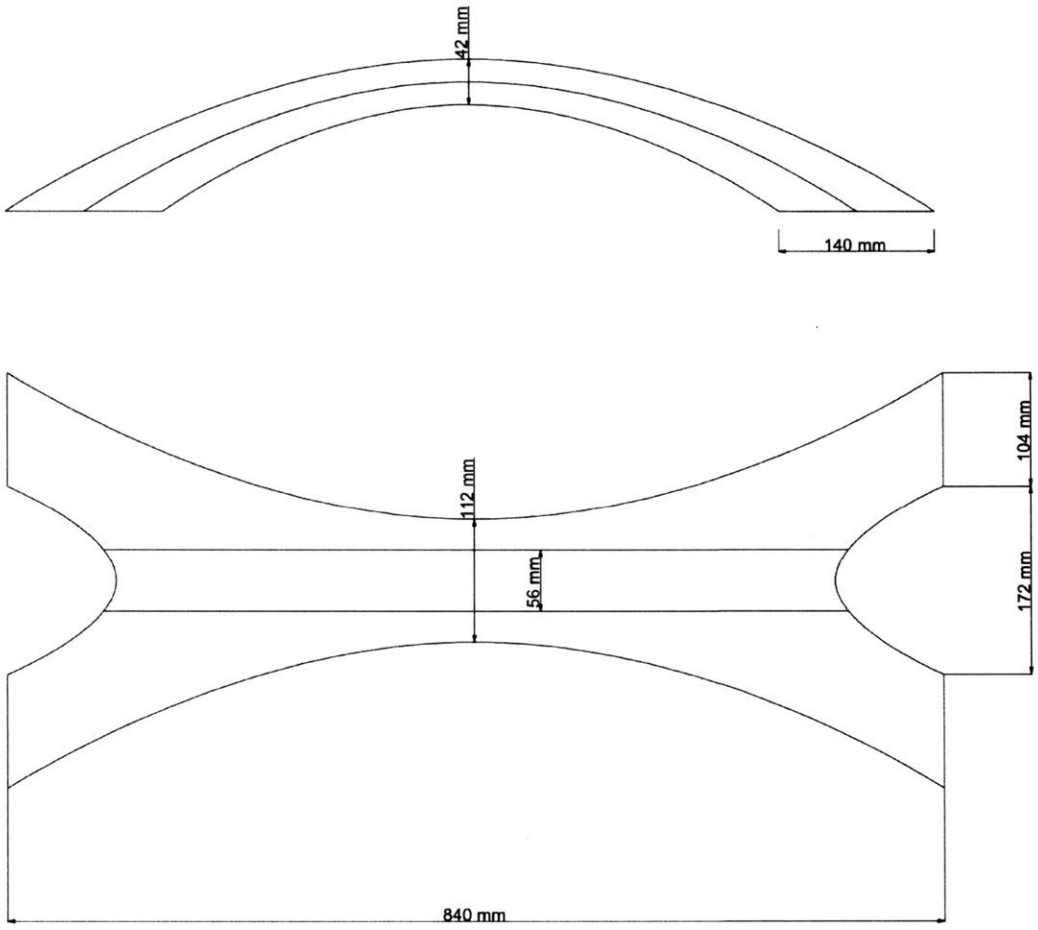

Figure 3.13 – 1:500 Scale model layer cuts to fit 3D printing considerations

As custom in Roman bridges in the 16th century and before, each arch opening has the voussoir radially cut outward and has a keystone at the crown (O'Connor 1993). In addition to radial cuts, a running pattern is utilized in elevation view such that the layers will interact with one another. The final voussoir design is shown in Figure 3.14.

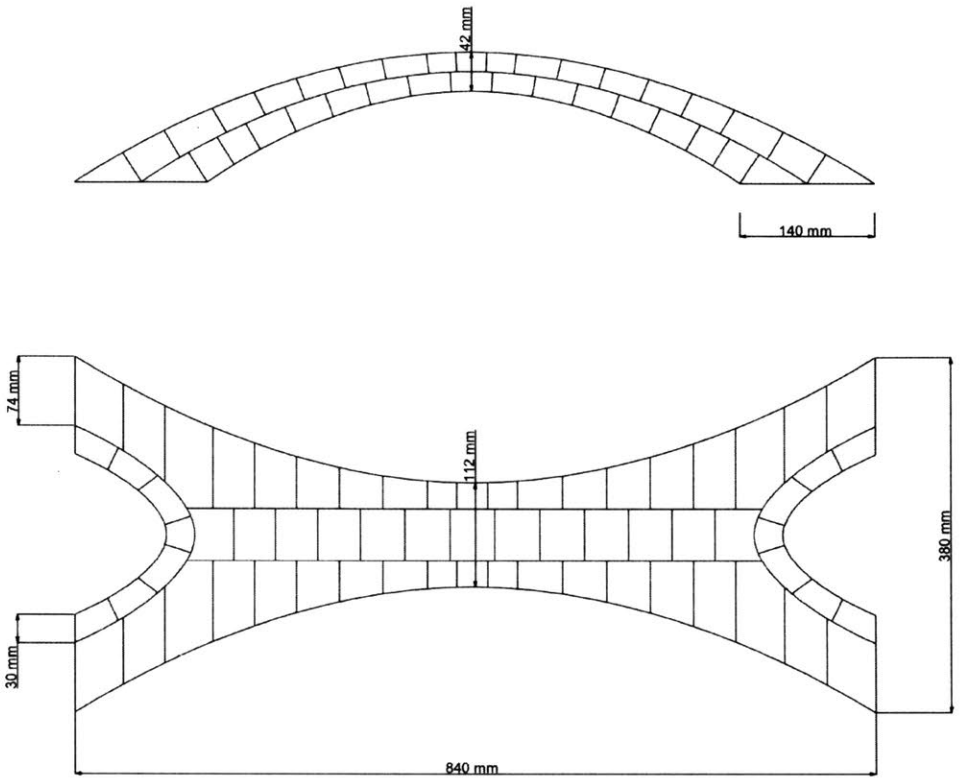

Figure 3.14 – 1:500 scale model radial cuts along all arch openings

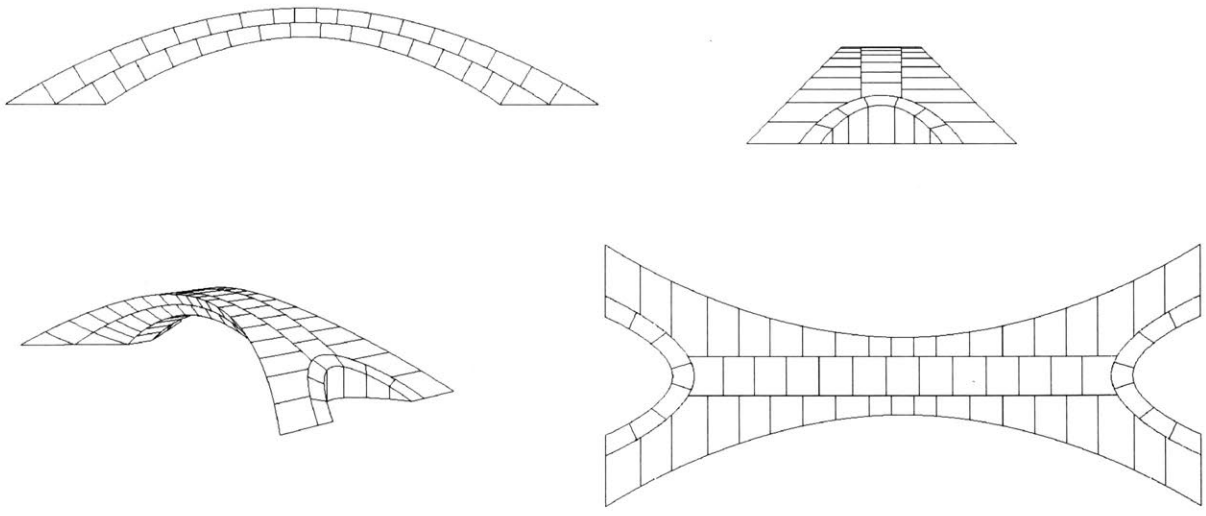

Figure 3.15 - Voussoir cuts of the bridge. Shown from left to right, top to bottom: (a) elevation view (b) side profile (c) isometric view (d) plan view.

The final voussoir design results in 126 solid 3D printed pieces. As the pieces are fragile when extracted, they are coated twice in a polyurethane spray for durability (Quinonez et al. 2010). Then, they are ready for assembly. In order for quick and accurate assembly, three vertical layers of rigid insulation are CNC-milled as temporary formwork for the scale model. Shown in Figure 3.16 are the pieces held in place by the temporary formwork.

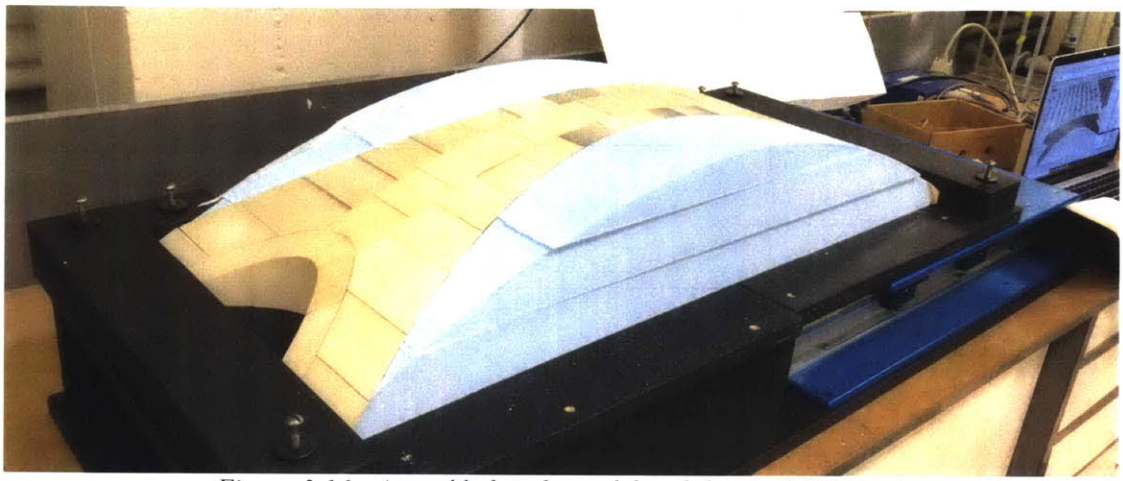

Figure 3.16 - Assembled scale model with layered formwork

Once the pieces are in the proper place, the formwork is removed, and the pieces remain in place. Shown below in Figure 3.17 is the assembly of all 126 pieces held together by compression. With no mortar or mechanical connections between the blocks, this physical model follows the classical no-tension hypothesis for masonry.

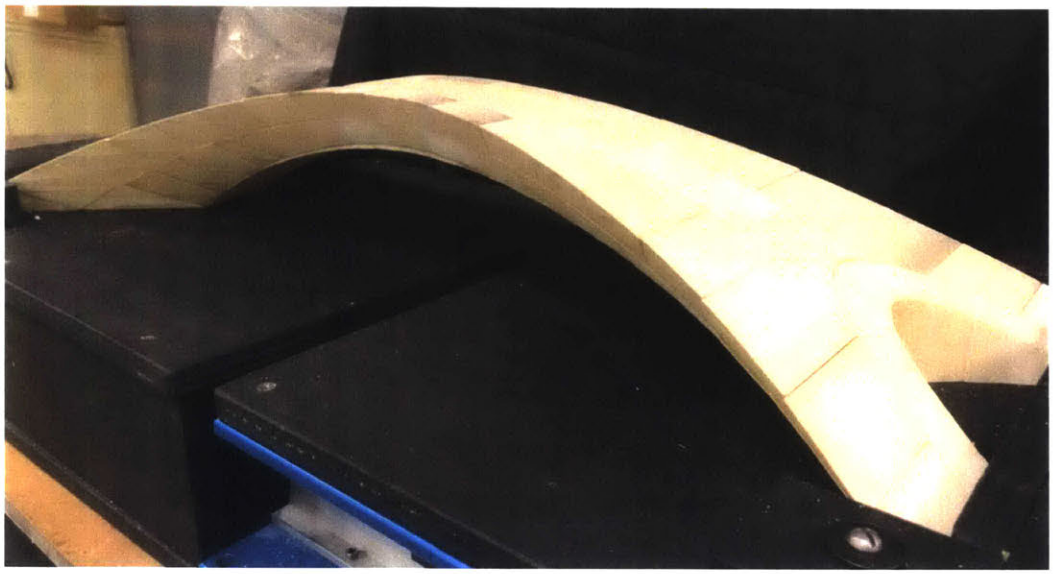

Figure 3.17 – Assembled 126 pieces with removed mold

Shown in Figure 3.17, the model demonstrates that the geometry for Leonardo's bridge over the Golden Horn is structurally stable.

Spreading Supports

In regard to the spreading support, an earthquake shake table is placed under one of the abutments. Only the "jog" function is utilized in order to control the constant speed at which the moveable abutment displaces horizontally. In addition, high-speed video is utilized to capture the collapse mechanism.

Three bridge collapses were done, and the change in horizontal displacements were measured manually with a digital caliper. The results are tabulated below in Table 3.9.

Table 3.9 – Recorded horizontal displacements at complete collapse

Trial	x (mm)
1	33.0
2	31.5
3	27.9
Average	30.8

The kinematic mechanism is observed in Figure 3.18 at four different stages throughout the collapse.

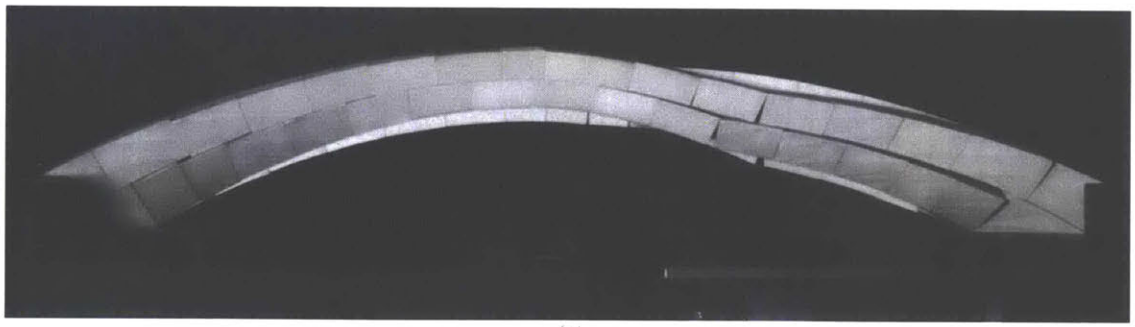

(a)

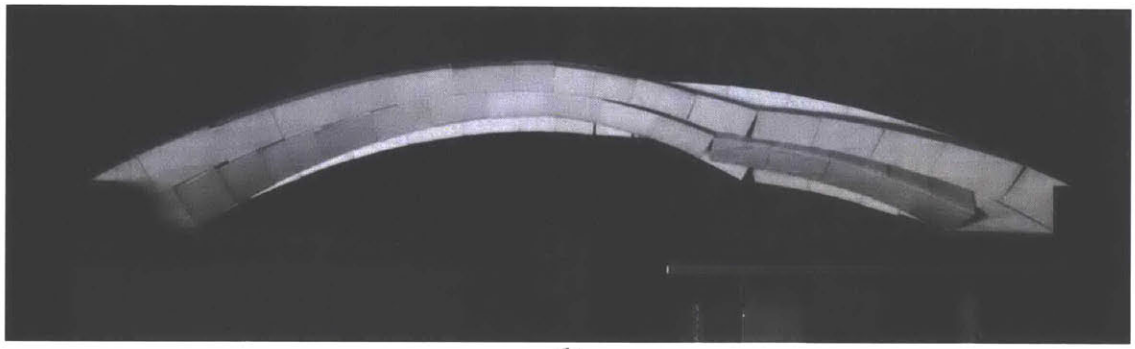

(b)

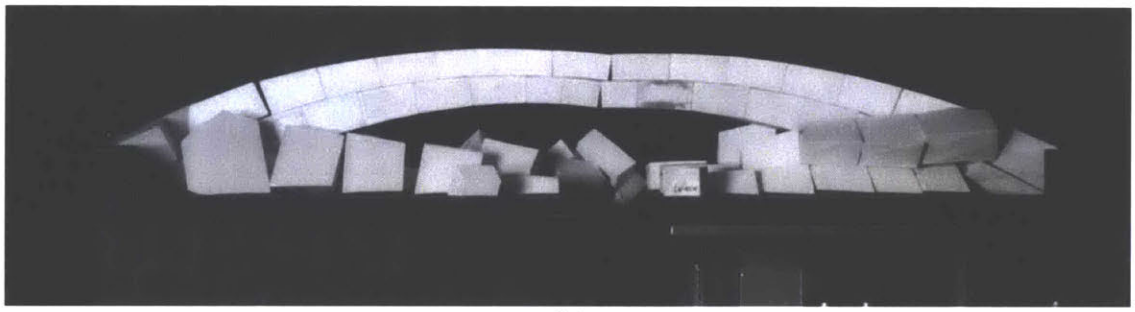

(c)

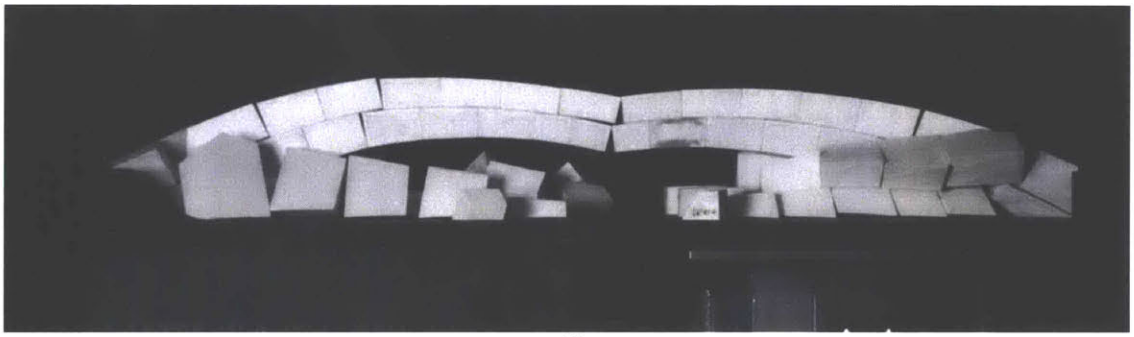

(d)

Figure 3.18– Kinematic mechanism of Trial 2. (a) first hinge (b) right before the side-arch collapse (c) right after the side-arch collapse (d) right before the central arch collapse

In comparison to the predicted kinematic mechanism, the bridge behaved in a more complex fashion than expected in four ways: the side arches acted independent of the central arch and collapsed first, the side arches hinged in an asymmetrical manner, the top and bottom layers of both the side arches and the central arch acted seemingly independently, and the hinge locations moved for the central arch.

The independent collapse of the side arches is a clear product of the voussoir cut. Since the side arches were not interlocked with the central arch, the bridge collapse is made of the independent action of the side arches and the central arch.

As shown in Figure 3.18 (a) and (b), the first intrado hinge of the side arch occurred at the abutment, but the extrado hinge did not occur at the crown as predicted. This could have occurred due to high stresses at the crown leading the extrado hinge to move down or rounded edges in the 3D printed voussoirs from damage during repeated testing. After the extrado and intrado hinges formed, the collapse followed a rigid body deformation as predicted.

After the collapse of the side arches, the central arch still stood. Shown below in Figure 3.19 (a) is the central arch when it first hinged in isolation from the side arches.

The top and bottom layer of the central arch worked independently, but for both layers the extrado hinge occurred at the crown. Due to the keystone, the hinge formed was asymmetrical. For the bottom layer, the intrado hinges occurred at the abutments, as predicted.

The hinge locations for the bottom layer of the central arch are circled in Figure 3.19 (b). The vertical voussoir cut at the fixed abutments prevented the hinge from forming there by impeding the rotation.

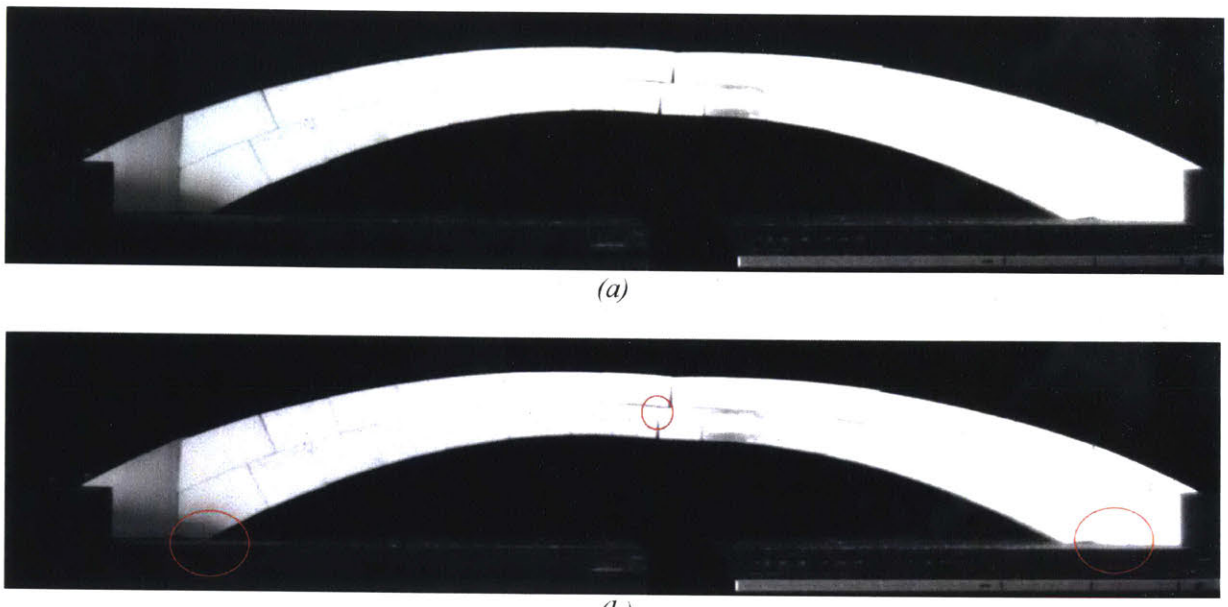

(a)

(b)

Figure 3.19– First hinges of central arch with spreading supports

After the right abutment continued to move, the hinges of the bottom layer relocated one voussoir and the top layer rested atop. The new hinge locations for the bottom layer of the central arch are circled below in Figure 3.20 (b). Some of the voussoir on the top layer were no longer touching and served as load for the bottom arch.

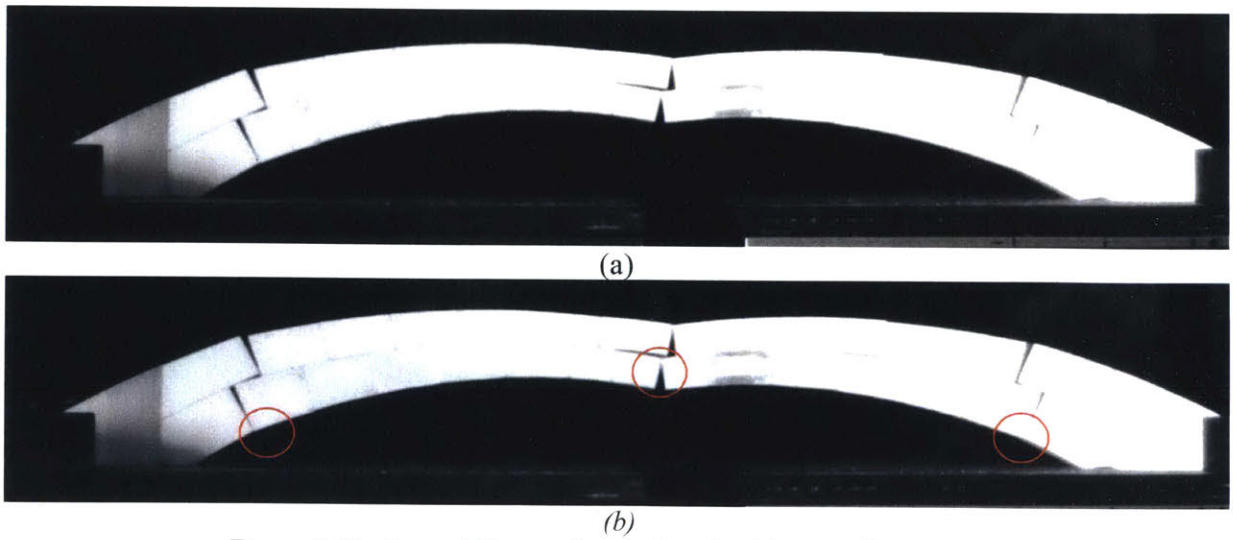

(a)

(b)

Figure 3.20– Second hinges of central arch with spreading supports

Right before collapse of the central arch, the left intrado hinge of the bottom layer moved over one voussoir and then the arch followed a rigid body deformation until complete collapse.

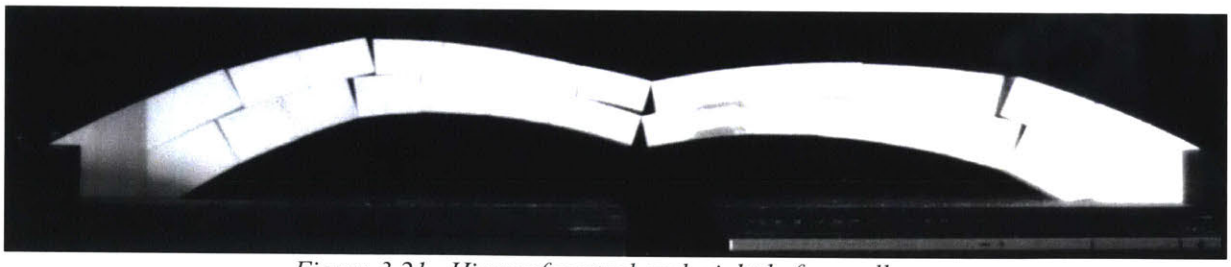

Figure 3.21– Hinge of central arch right before collapse

The allowable displacement before collapse was therefore smaller than predicted due to intrado hinges of the bottom layer moving closer to the crown as the abutment spread apart. The hinges at the support moved up due to the increase in thrust, and similarly stress, at the supports. While the hinge location changing was predicted for the full-scale bridge, it was not predicted for the 1:500 scale model. This is because it was assumed that the stresses would be very low in the model, but through the collapse of the model it is evident that this assumption is not precise.

In summary of these results, it is clear that the kinematic mechanism of Leonardo's bridge is significantly more complicated than predicted. The chosen voussoir cut affected the independent behavior of the side arches and the central arch along with the hinge locations. The side arches both collapsed in an asymmetric manner, where the location of the extrado hinge was far from the crown. For both the side arches and the central arch, the bottom and top layer acted independently of one another. It was found that the voussoir cut significantly affected the kinematic mechanism and that the increasing stresses at the hinges caused their locations to move. All of these factors contributed to an allowable displacement lower than predicted.

3.3 – Geotechnical Study

It is important to check the intended site of the bridge to see if the soil can properly support the bridge. This is done by understanding the Renaissance technology of the time to see what foundation solutions were available to connect the bridge with the ground, understanding the forces that would have been applied to the foundations and their geometry, and checking the soil properties that the foundations would bear on.

Foundation Precedents

As seen in the earlier section, uneven settlements of the supports of masonry arches can have severe impacts on their stability. Therefore, it is imperative that the supports experience minimal settlements, which nowadays is typically achieved through foundations bearing on stiff soil or rock. In the common occasion stiff soil or rock is buried under weaker soil, deep foundations can be used to access it. But deep foundations require technology such as motorized drills that were not available until well after Leonardo's time. On the other hand, shallow foundations were used for many bridges, such as the Rialto Bridge from 1340 shown in Figure 3.22.

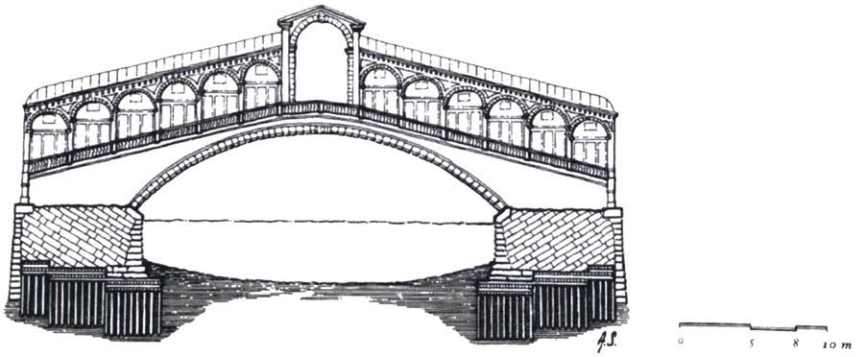

Figure 3.22 – Foundations of the Rialto Bridge, Venice from 1340 (Mark 1993)

The Rialto bridge from 1340 is used as a precedent for the foundation design of Leonardo's bridge for three reasons: the technology used in 1340 was still available in 1502, Leonardo would have been aware of this technology as the Rialto bridge is located in Venice, and the layers of the arch in the Rialto bridge are radially cut.

In addition to analyzing precedent foundations, Alberti recorded typical methods to design and build foundations in his well-known *The Art of Building in Ten Books* from the 15th century. For

foundations lying on less than stiff soil, Alberti recommends builders of his time to "dig a wide trench and to strengthen both of its sides with stakes, wickerwork, planks, seaweed, mud, and any similar materials to prevent the water from seeping in" (Alberti 1988). As Alberti refers to water seeping in, it is appropriate to assume this technique can be applied to digging beneath the water line.

From the Rialto bridge as precedent, Leonardo's bridge would likely utilize shallow rectangular footings as foundation for the bridge.

Forces on the Foundation

The loading on the foundation is dependent on the force flow throughout the bridge. As seen in Chapter 3.2, the weight of the structure requires a vertical and horizontal force to reach equilibrium. The vertical reaction is due to both the weight of the bridge over the water and voussoir that bear directly on the foundations. The horizontal reaction is due to the thrust from the voussoir over the water. In Chapter 3.2 both brick and stone were analyzed, but the bridge is only feasible in stone due to the high material stresses. The forces required for the stone bridge to in equilibrium are shown below in Figure 3.23-24 and tabulated in Table 3.10.

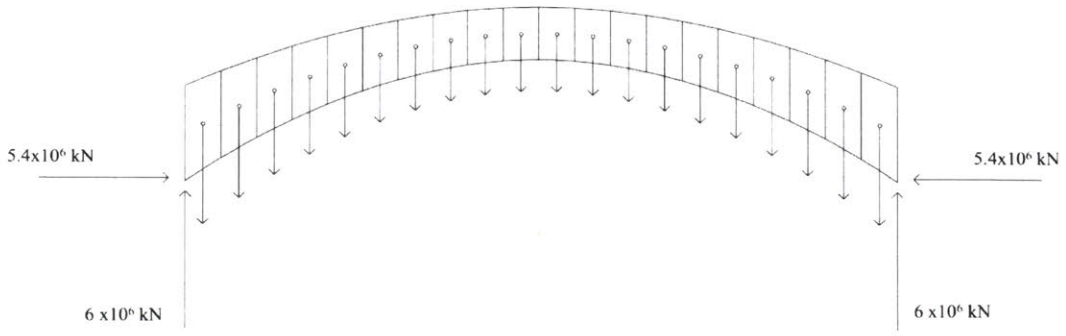

Figure 3.23 – Reactions needed at foundation for equilibrium of stone bridge

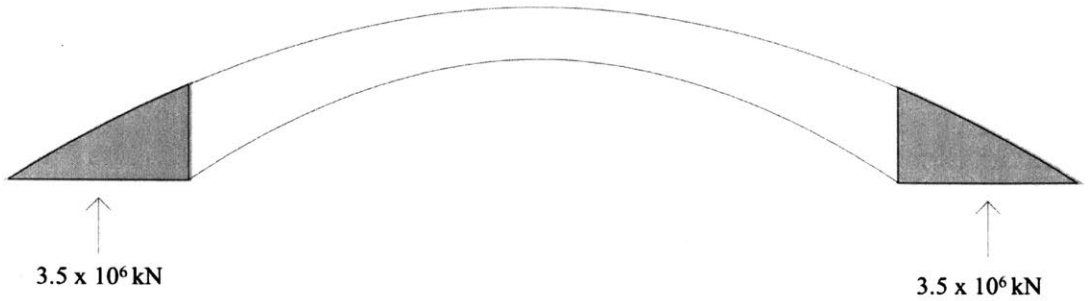

Figure 3.24 – Reactions needed at foundation for equilibrium of stone voussoir that bear directly on foundations

Table 3.10 – Reactions at each foundation for equilibrium of stone bridge

Reaction Orientation	kN
Vertical	$9.5x10^6$
Horizontal	$5.4x10^6$

An iconic feature of Leonardo's bridge is the arches at the abutments. While these arches may add to the aesthetic of the bridge, these arches help distribute the forces to the foundation. The arches at the abutments bear on the ground, which allow the weight of the bridge to be supported by the area of the footing. On the other hand, the arches at the abutments distribute the horizontal thrust force into a two-dimensional force. In consideration of how the forces are distributed at the abutment, and the rectangular nature of the footings, the following foundation plan is proposed in Figure 3.25.

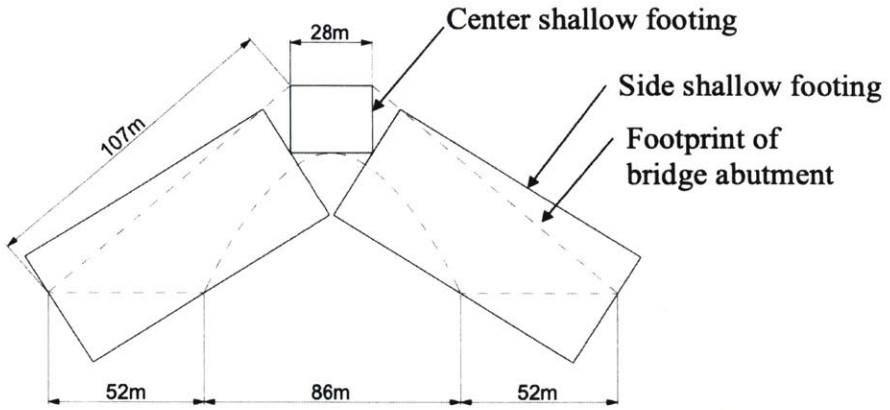

Figure 3.25 - Shallow foundation plan view

The proposed shallow foundation plan in Figure 3.25 shows a center shallow foundation and a side shallow foundation on either side. The arrangement is such that the two side foundations can be rotated to fit their local axis to the two-dimensional horizontal force shown in Figure 3.26, where V_1 is the vertical force on the center shallow foundation, V_2 is the vertical force on the side foundation, and H_2 is the two-dimensional horizontal force on the side foundation.

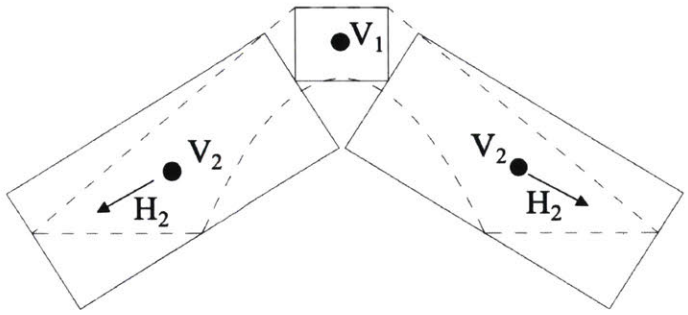

Figure 3.26 - Orientation of loading on shallow foundations in plan view. The solid dots indicate a force in the gravity direction and the arrows indicate in-plane thrust forces.

This orientation allows each footing to be loaded in a single plane: one vertical force and one horizontal force along the axis of the footing. It is important to note that the location of these forces may not result at the foundation's geometric centroid.

Soil Properties at the Site

Since the available technology in the 16th century calls for shallow foundations, the soil directly below the surface near the Golden Horn is of interest. In particular, the bearing capacity of the soil will determine the allowable pressure and the stiffness properties will determine the amount the foundations will settle. Furthermore, geological conditions of Istanbul in particular have been studied due to its abundance of cherished historical structures and its approximation to North Anatolian Fault Zone as shown in Figure 3.27 (Undul and Tugrul 2006).

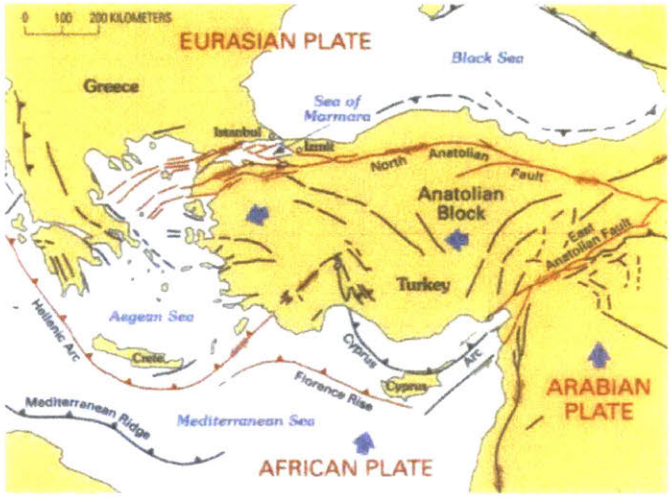

Figure 3.27 – Fault lines near Istanbul (Undul and Tugrul 2006)

As such, there is an understanding of the expected soil conditions at the intended site for the bridge and Undul and Tugrul (2006) describe of some of the geological conditions in Istanbul. They report of alluvium near the banks of the Golden Horn that is classified as a silty clay that is 42% CL, 37% CH, 10% MH, 4% CL –ML, and 7% ML (Undul and Tugrul 2006). While the bearing capacity of the alluvium near the Golden Horn is not explicitly stated, it is mentioned that it is very low.

Following a soil report from Togrol about the New Galata Bridge in Istanbul, the following properties for the alluvium, a slightly sandy clayey silt, are obtained:

$$c' = 0 \; ; \; \phi' = 19 \; ; E = 1{,}341\text{-}101{,}618 \; kPa \; (Togrol \; 2001)$$

The soil profile of the site is shown below, where the alluvium is covered in artificial fill and supported by greywacke (Togrol 2001). As the artificial fill is likely to have been placed after the 16th century, the alluvium is the top soil of interest.

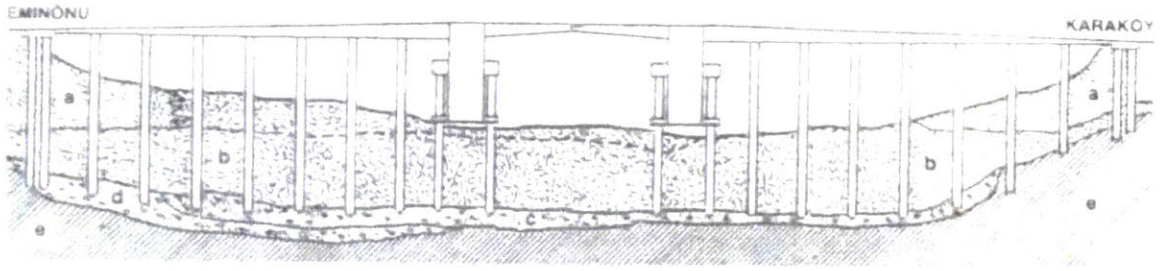

Figure 3.28 – Soil profile of the New Galata Bridge (a) Man-made fill (b) alluvium (c) cobbly gravel (d) weathered shale (e) sandstone/limestone/greywacke (Togrol 2001)

The properties of the alluvium near the Golden Horn found by Undul and Tugrul in 2006 compared to the properties listed by Togrol in 2001 are seemingly contradicting; the alluvium is classified as a silty clay, but it has no coefficient of cohesion.

Since the soil conditions are the site are not precisely known, and the bearing capacity of the alluvium is stated as "very low," it is non- trivial to determine if the soil is strong enough and stiff enough to support Leonardo's bridge. Although the strength and stiffness of the soil at the Golden Horn is out of the scope of this thesis, it would be useful for future work to address these challenges.

Chapter 4 - Conclusions and Future Work

Through Leonardo's written letter to the Sultan of Turkey and the sketch and a translation of his annotations in his folio, it is understood that the bridge intended to span 280 m over the water, 420 m from end to end, with a clear height of 49 m and minimum width of 28 m over the Golden Horn in modern-day Istanbul, Turkey.

After a structural analysis, it was found that the bridge is only feasible if made of stone and not brick due to the unusually high stresses at the crown of the bridge. It was predicted that the bridge would undergo a three-hinge kinematic mechanism when one abutment displaces 33 m. Similarly, for the 1:500 scale model it was predicted that the supports could withstand a horizontal displacement of 66 mm before collapse. Both of these predictions are an upper limit on the theoretically possible displacements since collapse would occur long before due to material crushing and nonlinear foundation behavior. For future work, it would be useful to use more complex computation tools to analyze the thrust line of the bridge in a more three-dimensional manner.

From the 1:500 scale model, it was evident that the bridge is structurally stable under its own self-weight. Under three spreading support experiments, the bridge collapsed at 33.0 mm, 31.5 mm, and 28.0 mm. The kinematic mechanism was more complex than the symmetric three-hinge mechanism predicted. The chosen voussoir cutting pattern affected the kinematic behavior by allowing the side arches and middle arch to act independent of each other. Additionally, the voussoir cuts prevented rotation at the predicted hinge locations for the central arch. From the hinge locations at the spring of the central arch moving up, it was evident that there were high stresses in the 1:500 scale model, which caused the hinge locations to change. To gain a more accurate collapse prediction for the scaled model an analysis of just the side arches should be done along with considerations of changing hinge locations. Additionally, it would be interesting to cut the voussoir in a different manner to engage the entire bridge in a single collapse.

Through a geotechnical study, it was found that there is alluvium soil near the surface of the Golden Horn. From literature it was discovered that this alluvium has a low bearing capacity, but there is still a need to determine the exact properties of the soil at the intended site. For future work, it

would be useful to test the soil at the Golden Horn to check if it is strong enough and stiff enough to support Leonardo's bridge.

In this thesis, the geometry of Leonardo's design was interpreted, and found to be structurally feasible with the material available at the time.

Chapter 5 – Appendices

Appendix A: Excerpt from *The Literary Works of Leonardo Da Vinci Commentary* by Carlo Pedretti and Jean Paul Richter 1977:

"Copia d'una lettera che l'infedele di nome Lionardo trasmise da Genova.
Io, Vostro servo, riflettendo sino adesso sulla faccenda del mulino, con l'aiuto di Dio, ho trovato una maniera per cui, con un artificio, costruirò un mulino [che funzioni] senza acqua, soltanto con il vento, in modo che si faccia con meno [di quanto] un mulino in mare; e non solo sia pure piu agevole per la gente ma anche sia [adatto per] in qualsiasi luogo.
Inoltre Iddio (che sia esaltato!) mi ha concesso di estrarre l'acqua dalle navi con un artificio, senza funi o corde, con una machina idraulica che gira de sè.
Io, Tuo servo, ho sentito dire che Vi siete proposto di costruire un ponte da Stambul a Galata, ma non l'avete fatto perché non si trova un uomo capace. Io, Tuo servo, lo so. Io [lo] eleverò alto quanto un edificio sì che nessuno acconsenta di passarvi sopra, per quanto sarà alto. Ma ho pensato di fare uno sbarramento, di togliere dopo l'acqua, e di conficcare i pali. Farò in modo che da sotto possa uscire perfino una nave con la vela [spiegata]. Farò un ponte levatoio in modo che, quando si vuole, si possa passare sulla costa di Anatolia. Ma siccome l'acqua scorre in continuazione, le sponde sono erose. Perciò faro un artificio in modo che quelle acque scorrano, scorrendo al fondo non rechino danno alla sponda. I sultani tuoi successori potranno farlo con poca spesa.

Se Dio vuole presterete fede a queste parole e darete comandamento considerando codesto servo sempre al Vostro Servizio.
Questra lettera è stata scritta il tre di luglio.
E` di quattro mesi.

Copy of a letter that the infidel by the name of Leonardo has sent from Genoa.
I, your servant, having thought for some time about the matter of the mill, with the help of God, have found a solution, so that, with an artifice, I will build a mill which works without water, but only by the wind in a way that it will take less than a mill at sea; and not only would it be more convenient to the people, but it would also be suitable to any place.
Furthermore, God (let him be exalted!) has granted me to find a way of extracting the water from the ships without ropes or cables, but with a self-operating hydraulic machine.
I, your servant, have heard about your intention to build a bridge from Istanbul to Galata, and that you have not done it because no man can be found who would be able to plan it. I, your servant, know how. I would raise it to the height of a building, so that, on account of its height, no one will be allowed to go through it. But I have thought of making an obstruction so as to make it possible to drive piles after having removed the water. I would make it possible that a ship may pass underneath it even with its sails up. I would have a drawbridge so that, when one wishes, one can pass on to the Anatolia coast. However, since water moves through continuously, the banks may be consumed. Thus I may find a system of guiding the flow of the water, and keep it at the bottom so as not to affect the banks. The sultans, your successors, will be able to do it at a little expense.
May god make you believe these words and make you consider this servant of yours always at your service.
This letter was written the 3rd of July. It is four months old."

Appendix B: References

Alberti, Leon Battista. 1988. *On the Art of Building in Ten Books*. Translated by Joseph Rykwert, Neil Leach, and Robert Tavernor.

Allen, Edward, Waclaw Zalewski, and Boston Structures Group. 2010. *Form and Forces*. John Wiley & Sons, Inc.

Bertolesi, Elisa, Gabriele Milani, Fulvio Domenico Lopane, and Maurizio Acito. 2017. "Augustus Bridge in Narni (Italy): Seismic Vulnerability Assessment of the Still Standing Part, Possible Causes of Collapse, and Importance of the Roman Concrete Infill in the Seismic-Resistant Behavior." *International Journal of Architectural Heritage* 11 (5): 717–46.

Kayra, Cahit. 1990. *İstanbul haritaları : Ortaçağdan günümüze*. Türkiye Sınaî Kalkınma Bankası.

Cardarelli, Fracois. 2003. *Enclyclopaedia of Scientific Units, Weights and Measures*. Translated by M.J. Shields. Springer.

Heyman, Jacques. 1969. "The Safety of Masonry Arches." *International Journal of Mechanical Sciences* 11: 363–85.

Heyman, Jacques. 1995. *The Stone Skeleton*. Cambridge University Press.

Isaaccson, Walter. 2017. *Leonardo Da Vinci*. New York, NY: Simon & Schuster.

Ispir, Medine, and Alper Ilki. 2013. "Behavior of Historical Unreinforced Brick Masonry Walls under Monotonic and Cyclic Compression." *Arabian Journal for Science and Engineering* 38 (February). https://doi.org/10.1007/s13369-013-0567-4.

Leonardo da Vinci. 1497. "Manuscrit L." Paris, Library of the Institut de France.

Mark, Robert. 1993. *Architectural Technology up to the Scientific Revolution*. Massachusetts Institute of Technology.

Moropoulou, Antonia, Ahmet Cakmak, and Kyriaki Polikreti. 2002. "Provenance and Technology Investigation of Agia Sophia Bricks, Istanbul, Turkey." *Journal of the American Ceramic Society* 85 (2): 366–72.

Nicholl, Charles. 2004. *Leonardo Da Vinci Flights of the Mind*. Penguin Group.

Ochsendorf, John Allen. 2002. "Collapse of Masonry Structures." Dissertation, University of Cambridge. https://www.repository.cam.ac.uk/handle/1810/244820.

Ochsendorf, John Allen. 2006. "The Masonry Arch on Spreading Supports." *The Structural Engineer* 84 (2): 29–36.

O'Connor, Colin. 1993. *Roman Bridges*. Cambridge University Press.

Pedretti, Carlo, and Jean Paul Richter. 1977. *The Literary Works of Leonardo Da Vinci Commentary*. Vol. 2. University of California Press.

Quinonez, Alvaro, Jennifer Zessin, Aissata Nutzel, and John Allen Ochsendorf. 2010. "Small-Scale Models for Testing Masonry Structures." *Advanced Materials Research* 133–134: 497–502.

Schettini, Franco. 1972. "Parametro" 10: 68–79.

Shapiro, Elaine Elizabeth. 2012. "Collapse Mechanisms of Small-Scale Unreinforced Masonry Vaults." Master of Science in Building Technology, Massachusetts Institute of Technology.

Togrol, E. 2001. "Golden Horn: A Historical Survey of Geotechnical Investigations."

Undul, Omer, and Atiye Tugrul. 2006. "The Engineering Geology of Istanbul, Turkey." *The International Association for Engineering Geology*.

Venerella, John. 1999. *The Manuscripts of Leonardo Da Vinci in The Institut de France - Manuscript L*. Milano.